NASA CONTRACTOR REPORT

NASA CR-463

CONTRIBUTION OF COMBUSTION NOISE TO OVERALL ROCKET EXHAUST JET NOISE

by Loren E. Bollinger, E. Stokes Fishburne, and Rudolph Edse

Prepared under Contract No. NAS 8-11150 *by*
THE OHIO STATE UNIVERSITY
Columbus, Ohio
for George C. Marshall Space Flight Center

NATIONAL AERONAUTICS AND SPACE ADMINISTRATION - WASHINGTON, D. C. - MAY 1966

NASA CR-463

CONTRIBUTION OF COMBUSTION NOISE TO OVERALL ROCKET EXHAUST JET NOISE

By Loren E. Bollinger, E. Stokes Fishburne, and Rudolph Edse

Prepared under Contract No. NAS 8-11150 by
THE OHIO STATE UNIVERSITY
Columbus, Ohio

for George C. Marshall Space Flight Center

NATIONAL AERONAUTICS AND SPACE ADMINISTRATION

For sale by the Clearinghouse for Federal Scientific and Technical Information
Springfield, Virginia 22151 – Price $3.00

FOREWORD

This technical report was prepared by Loren E. Bollinger, E. Stokes Fishburne, and Rudolph Edse of The Ohio State University, Department of Aeronautical and Astronautical Engineering, Rocket Research Laboratory, under Contract NAS8-11150. Chief investigators of the experimental and theoretical phases, respectively, were Assistant Professors Loren E. Bollinger and E. Stokes Fishburne. Professor Rudolph Edse was supervisor of the research project. The contract was monitored by Dr. G. H. R. Reisig of the Test Laboratory, Marshall Space Flight Center, National Aeronautics and Space Administration, Huntsville, Alabama.

Significant contributions were made by Mr. James A. Laughrey, Mr. Jerome W. Pliickebaum, and Mr. Clinton DeWorth.

TABLE OF CONTENTS

LIST OF FIGURES

LIST OF FIGURES (CONT'D)

LIST OF FIGURES (CONT'D)

SECTION I

INTRODUCTION

In recent years, considerable effort has been devoted to the study of aerodynamic noise. The study of aerodynamically-generated noise has become one of the more interesting and yet frustrating areas of science. Aerodynamically-generated noise generally is classed as that noise generated by the interaction of a moving layer of gas with a gas at rest. Thus, we exclude from the area of aerodynamically-generated noise such phenomena as shock waves and the accompanying sonic boom. Of particular interest is the noise generated by the interaction of a high-velocity jet with a quiescent or ambient atmosphere. The magnitude of the aerodynamically-generated noise may vary many fold. On the one hand we have the noise which may be generated by slightly opening a cylinder containing high-pressure air to the atmosphere. This motion of the high-pressure air into the atmosphere generates a fairly small amount of noise depending on the velocity. At the other extreme we have the noise generated by one of the large rockets such as the Saturn 1.5-million-pound-thrust rocket engine (F-1). The noise generated by this rocket is so intense that it is potentially damaging to the human physiology and to various structures surrounding the area.

The purpose of this particular investigation was twofold in nature. First, attempts were to have been made to determine the origin of the very low frequency noise, less than 100 cycles, associated with the Saturn rocket engine and secondly, to investigate various techniques for externally suppressing the noise of the Saturn rocket. The importance of the

second phase is obvious, particularly in view of future plans to fire still larger rocket engines at the test facility. However, to investigate various techniques for suppressing the noise properly, we must first determine the actual origin of the noise. Thus the study of this problem is divided very clearly into the two phases of determining the origin of the noise and attempting to suppress it.

SECTION II

THEORETICAL BACKGROUND

INTRODUCTION

The noise emitted by the interaction of a high-velocity gas jet with the ambient atmosphere has been the subject of many investigations. References 1 through 10 list only a few of the research efforts undertaken. Reference 11 presents a bibliography of research devoted to the study of noise. Most of the current theories concerning the generation of noise by the interaction of a gas jet and the ambient atmosphere begin with the fundamental theory as developed by Lighthill (Ref. 1, 2, and 5). In view of the many reports and papers discussing the mathematical theory for the generation of noise, we will review only the basic assumptions and results.

In principle, when a jet of gas passes through an orifice into an ambient atmosphere, the flow within the jet probably is laminar at the exit of the orifice. When a high-velocity gas stream enters the surrounding atmosphere, enormous stresses are established between the gas jet and the ambient atmosphere. The stresses set up at the so-called

shear layer increase as the jet velocity increases. Due to the enormous shear forces, the laminar shear layer rapidly becomes turbulent. In fact, the mixing region between the gases of the laminar jet and the ambient atmosphere becomes completely turbulent within approximately one-half the nozzle diameter from the orifice. The mixing region continues to spread and eventually a laminar jet no longer exists. This condition of mixing is essentially the same for subsonic and supersonic jets with the noted exception that as the velocity of the jet increases the interaction becomes more violent.

In his study of noise generation by the shearing action between a gas jet and the ambient atmosphere, Lighthill distinguished between the subsonic and supersonic jets in the following manner. The Mach number of the jet was determined as the ratio of the jet velocity to the speed of sound of the ambient atmosphere. Hence, if the jet were very hot, although the jet may be subsonic with respect to its high-temperature gases, it could be supersonic with respect to the ambient atmosphere. In addition to considering the noise generated by subsonic and supersonic jets, we also are interested in the propagation of the radiation. In the study of noise propagation we find it advantageous to divide the radiation field into two regions called the near field and the far field. The near field is defined as that area within approximately one wave length of the source. The far-field, on the other hand, is that region in which the pressure variations decrease inversely as the distance from the source increases. Because of physical limitations, the measurements reported herein were obtained in the near field.

Lighthill has shown that the general characteristics of noise generated by the interaction of a gas jet and the atmosphere can be explained with a fair degree of success on the basis of a distribution of quadrupole sources. These sources are distributed within the mixing region and represent noise generation due to the turbulence. Thus, Lighthill basically assumes that the noise is produced by the action of a turbulent flow. With these assumptions, Lighthill was able to explain, fairly successfully, the dependence of the noise power on the eighth power of the jet velocity. Experiments, in general, agree with this velocity dependence quite well. These results were derived under the assumption of low Mach number flows.

Ribner (Ref. 4) has presented an excellent analysis of the generation of sound by turbulent jets. In addition to reviewing the sound generated by subsonic jets he discusses in some detail sound generated by supersonic jets. One of the more important aspects of his presentation is the dependence of the noise power of the supersonic jet on the third power of the jet velocity. This conclusion is in basic agreement with measurements made to date.

ACOUSTIC SOURCES

In studying possible origins of jet noise, we find that we can employ three classic sources of sound: a monopole source, a dipole source and a quadrupole source. A monopole source is analogous to a small sphere whose radius fluctuates with a given frequency. The rms pressure field may be represented as (Ref. 6)

$$p \approx \sqrt{\frac{\rho_o c_o}{\rho c}}\, U\, \rho\, c\, (Ka)\, \frac{a}{r}$$

where

p = pressure

ρ = the density near the source

ρ_o = the ambient density in the far field

c = the velocity of sound near the source

c_o = the velocity of sound in the far field

U = the rms value of the velocity of the surface of the sphere

a = the diameter of the sphere

r = the distance from the center of the sphere

K = the wave number = $2\pi/\lambda$

As indicated by Morgan (Ref. 6), the significance of the term Ka can be shown as follows

$$Ka = \frac{\pi f D}{c_o}$$

where f = frequency, and D = the diameter of the source. After a study of the jet noise from a number of rocket engines Eldred, et al (Ref. 12) have been able to show that the peak of the acoustic power occurs at the non-dimensional frequency

$$\frac{fDc}{U_c} \cdot \frac{a^*}{c_o} = 0.25$$

where

D_c = characteristic diameter of the flow

U_c = characteristic velocity of the flow

a^* = critical velocity of sound in the flow

Employing these two relations we find that a typical value of the product is approximately 0.8.

A dipole source can be pictured as a line along which a rigid sphere is oscillating back and forth. In the area of acoustics any force acting on the medium is generally equivalent to a dipole. The rms pressure, due to the dipole source, is given as (Ref. 6)

$$p = \sqrt{\frac{\rho_o c_o}{\rho\, c}}\ \frac{1}{2}\, U \left[\rho\, c\, (Ka)^2\right] \left[\frac{a}{r}\right] \left[1 + \left(\frac{1}{Kr}\right)^2\right]^{1/2} \cos\theta$$

where U = the rms velocity of the oscillating sphere and θ = the angle relative to the axis of the dipole. At this point we find that the assumption of dipole sources introduces a new factor into the discussion of the noise problem. The new factor is the angle or directivity of the noise. The directivity of the jet noise has been verified by some of the experimental studies indicated earlier.

The quadrupole source consists essentially of two opposing dipole sources. If the dipole sources are equal and opposite, similar to the normal pressure on a body, the source is called a longitudinal quadrupole. However, if the dipole sources act parallel to the sides of a body, then the source is called lateral quadrupole. It is this concept of a quadrupole source that led Lighthill to his fundamental theory concerning the origin of jet noise. The pressure variation can be given as (Ref. 6)

$$p = \alpha \sqrt{\frac{\rho_o c_o}{\rho\, c}}\, U \left[\rho\, c\, (Ka)^3\right] \left[\frac{a}{r}\right] \left[\left(2 + \frac{3}{(Kr)^2}\right)^2 + \left(\frac{2}{Kr}\right)^2\right]^{1/2} \sin\theta \cos\theta$$

The basic difference between a longitudinal quadrupole and a lateral quadrupole concerns the directivity of the noise. With a longitudinal quadrupole the directivity of the noise resembles that of a figure eight.

On the other hand, with a lateral quadrupole, the directivity of the noise resembles that of two figure eights at right angles to one another. From experimental evidence we find that the lateral quadrupole represents the directivity of rocket and jet exhaust noises quite well.

The basic theory for the generation of noise by subsonic and supersonic jets, as expounded by Lighthill and others, enables us to determine, in general, the acoustic efficiency, the directional distribution, the frequency spectrum and the dependence of jet noise on the jet velocity. These characteristics of jet noise are predicted on the basis of sound radiating from quadrupole sources located within the turbulent mixing region. No attempt has been made to include in the analysis noise which may arise from combustion instabilities or from the interactions between eddies and the shock waves formed in supersonic jets. One of the more striking aspects of this theory is the success with which the directivity of noise can be predicted.

ADDITIONAL NOISE PRODUCED BY CHEMICALLY REACTING GAS JETS

In view of the large effort devoted to the investigation of the nature and generation of jet noise it would appear that very little remains to be studied. However, such is not the case. Most of the studies to date have been restricted to jets of cold non-reacting gases. If we consider a jet of chemically-reacting species directed into a cool, oxidizing atmosphere, other sources of noise may arise.

The mixture ratio of the propellant of a rocket engine generally is such that the engine operates slightly fuel rich. It is a well-established fact that a rocket engine gives the best performance when

it is operating under slightly fuel rich conditions. Thus, it is inevitable, regardless of the degree of completion of the combustion process in the combustion chamber, that a fairly large amount of unreacted fuel radicals will be present in the exhaust jet.

The propellants in use at this time contain chemical species composed primarily of C, H, O, and N. If such a system were employed in a rocket engine operating fuel rich, we could expect various amounts of CO, CH, H, and other species in the exhaust. Since these species are highly reactive, they would react very quickly upon contact with the air and form CO_2 and H_2O. During the process of mixing and reacting with the air, a tremendous amount of energy is released. It is this explosive energy release outside the combustion chamber which could lead to rather intense low-frequency noise. Thus far, we have considered that unreacted radicals exist in the exhaust only because the rocket engine is operated fuel-rich. Large quantities of unreacted chemical species may exist in the exhaust jet when the propellant mixing process is inadequate in the combustion chamber. At this point we shall neglect the actual combustion process in the chamber and the dependence of the combustion process on the size and shape of the chamber. This aspect is neglected since we are interested primarily in the size and shape of the expansion nozzle and the expansion process.

To obtain chemical equilibrium at the nozzle exit we would need a very long nozzle with a very small divergence angle. A long nozzle with small divergence angle provides a longer residence time and reduces the temperature and pressure gradients which normally lead to nonequilibrium effects. Obviously, weight limitations make the use of a long nozzle

highly undesirable. However, as we begin to shorten the nozzle, and increase the divergence angle to maintain the same area ratio, we begin to obtain departures from chemical equilibrium. This situation arises since the gases, because of their high velocities, cannot react sufficiently rapid to maintain chemical equilibrium. As the divergence angle is increased still farther, we find that the composition at the nozzle exit begins to approach that existing at the throat of the nozzle. If the composition at the exit is the same as at the throat, we say that the gas is chemically frozen during the expansion process. In practice, the flow in the rocket nozzle is somewhere between these two extremes.

Since we have concluded that a high probability exists for substantial quantities of unreacted radicals to be present in the exhaust jet, we may only determine the manner in which these radicals react with the ambient atmosphere. We are neglecting the possibility of incomplete combustion in the combustion chamber and subsequent combustion of pockets of explosive gases upstream of the nozzle exit because of the additional complexity of the problem. The explosion or rapid combustion of these pockets of gases could lead to detonation waves and shock waves. Furthermore, as these pockets of gases move downstream and into the shock-wave structure in the exhaust jet, an acoustical disturbance would be produced. At this point it would be difficult to state exactly the nature of the acoustical disturbance.

In the study of the explosive release of energy due to rapid chemical reactions between the exhaust jet and the ambient atmosphere, major emphasis must be given to the manner of mixing between the gases of the

exhaust jet and the ambient atmosphere. At this time the theory of turbulent mixing is insufficiently developed to accurately predict the manner in which the jet and the surrounding air mix. However, a few statements can be made regarding the mixing process. It is fairly obvious that practically all of the mixing will occur at subsonic velocities as determined by the local gas temperature. This condition will exist since the surrounding air cannot be accelerated to supersonic velocities in the conventional arrangement and mixing cannot occur in which one component is supersonic and one component subsonic.

It is difficult to estimate the approximate Mach number of the resulting mixture. The general nature of the turbulent mixing implies mass interchange on a large scale. In the particular case of the interaction between a supersonic jet and the ambient atmosphere, we can expect the formation of eddies or vortices, similar to the von Karmen vortices, which tend to maintain their identity. It is within these vortices that explosive combustion may occur.

To determine the probability of an explosive combustion process or detonation wave within the vortex, we must know more about the probable composition of the exhaust gases. Furthermore, to correlate the generation of low-frequency noise with explosions within the vortices, we must determine the rate with which the vortex is moving in space and its rate of dissipation. Most important, however, is the question of whether the "noise" generated by the rapid combustion is due to explosive combustion (and the accompanying noise), due to the formation of detonation waves, or due to the energy release increasing the intensity of the turbulence and the resulting fluctuation of pressure and density. Eschenroeder

(Ref. 13) has investigated the intensification of turbulence due to chemical heat release in the wake of a projectile. However, Eschenroeder made the basic assumption that the Mach number of the mixture is small, which may not be the situation in this study.

Rather than proceed further into the theory of noise generation, we felt that it would be advantageous to conduct a few experiments to determine the nature of the noise generated and its frequency dependence. It was anticipated that some of the data collected would prove vital to the question of whether or not combustion between unreacted portions of the jet and the air could lead to the generation of low-frequency noise.

To determine the effect of various quantities of unreacted chemical species in the exhaust jet, one can conduct a series of experiments in which only the mixture ratio of the rocket engine would change. The measurements of the noise would be conducted with the microphones at a fixed location. If, as the mixture ratio became more rich, the noise shifted to the lower frequencies, we could conclude that the chemical reaction in the exhaust jet may have a predominant effect on the low-frequency noise. However, unless additional experiments were conducted, it would be difficult to separate the degree of the contribution from unreacted species in the exhaust jet from the contribution of the noise in the combustion chamber. In the limiting case where combustion takes place outside of the combustion chamber, the low-frequency noise probably would be the most pronnounced. Hence, the basic approach would be the investigation of the dependence of the low-frequency noise upon the mixture ratio of the rocket engine.

SECTION III

EXPERIMENTAL PHASE

INTRODUCTION

Experiments were conducted with a 500-pound thrust rocket motor wherein the noise generated by the exhaust jet was measured and analyzed for various operating conditions. Normally the rocket motors are fired in a horizontal position, or aimed slightly downward, in this Laboratory. Usually liquid-propellant motors are fired vertically down or near the horizontal position because of the danger of unburned propellant collecting in the combustion chamber during the starting phase. An explosion or detonation could occur during the ignition cycle if the propellant collected in the chamber and ignition were delayed or erratic.

In these experiments it was decided that the rocket motor should be fired vertically up in order to obtain a reasonably free field, from an interference standpoint, to make the noise measurements. The propellant employed was RP-1 and liquid oxygen. To avoid the propellant-collection problem in the combustion chamber during the ignition cycle, it was decided to use a strong pilot flame in the combustion chamber prior to the introduction of the primary fuel and oxidizer. Gaseous hydrogen and gaseous oxygen were selected. After the initial experiments were conducted, it was found that an adequate pilot flame could be produced by using gaseous hydrogen and liquid oxygen. When the flow of liquid oxygen was initiated during an experiment, the oxygen entered the combustion chamber in the gaseous state because of the initially-modest flow rates used and the necessity to cool down the liquid-oxygen line and the

injector. After the pilot flame was established, RP-1 was introduced and the flow rates of it and the liquid oxygen were increased to the final desired values. The flow of pilot hydrogen gas was terminated after the flow of RP-1 was established.

The noise produced by the rocket exhaust jet was measured with four special microphones located at various positions during the different experiments. These data were recorded on a multichannel tape recorder and a frequency analysis was performed later.

EXPERIMENTAL EQUIPMENT

Several small rocket motors, together with the associated flow control systems and instrumentation, were designed and fabricated for these experiments. Special equipment and sensors were installed to measure and analyze the noise produced by the exhaust jet. Measurements were made during various operating conditions of the rocket motor; the primary parameter employed was mixture ratio.

The general arrangement of the experimental facilities is shown in Fig. 1. Normally the rocket motors are fired in the concrete test pit, which has 18-inch reinforced walls. However, for these noise studies, it was decided to mount the rocket motor outside to minimize reflections of the sound waves from the walls. Strong interference patterns would have been set up had the motor been mounted inside.

An air-conditioned instrumentation trailer was used for the tape recorder and pen-writing oscillograph location. Also, the noise analysis equipment was located in this trailer which was situated well away from the rocket-motor position.

Details of the various subsections of the rocket motor installation and the noise analysis equipment are given in the following sections.

Rocket Motors

The rocket motor system installed was designed for a maximum of 500 pounds of thrust for a duration as long as six minutes. The fuel and oxidizer were selected to be the same as those used in the Saturn series of rocket engines for the first stage. The fuel, RP-1, was procured in accordance with military specification MIL-R25576B. A bulk facility for liquid oxygen was installed for use on this research program. Bulk quantities of liquid oxygen were delivered to the laboratory by a truck tanker under contract from the supplier, as shown in Figure 2.

Figures 3 and 4 illustrate the general arrangement of the test-pit area. Mirrors were used to observe the motor during firing operations, as can be seen in Figure 3. During the experiments, the operator could obtain a visual check of the various pressures and so forth by observing the status panel in the firing pit. Data used for performance calculations were recorded in the instrumentation trailer.

A number of injectors and variations on the basic injector designs were employed during the various experiments. Details of the injectors are shown in Figures 5 through 9. Pertinent dimensions are shown. The basic spray patterns are the same for each type of injector. A multiple impinging stream type was employed so that changes in the total flow rate and in the mixture ratio would not change the stream direction inside the combustion chamber. With this arrangement, the resultant momentum is always axial thereby minimizing the probability of burning through the wall of the combustion chamber. The impingement

point in front of the injector was changed in the different designs.

The copper combustion chamber insert is illustrated in Figure 10. For some of the experiments, a larger value of characteristic length, L*, was desired. For this purpose replaceable exhaust nozzle inserts were utilized. These are shown in Figures 11 and 12. These could be silver-soldered into the copper chamber. Small static pressure taps were located at the end of the exhaust nozzle to permit measurement of this pressure. Values were measured by an electrical transducer and recorded on the pen-writing oscillograph. In addition, another measurement was made with a differential-pressure indicator which was located on the status panel in the firing pit.

Coolant jackets for the copper combustion chamber are illustrated in Figures 13 and 14. Later in the experiments, it was decided to increase the residence time of the propellant mixture by adding on a section to the combustion chamber as illustrated in Figures 15 and 16.

Several views of the rocket motor, with the extension on it, are depicted in Figures 17 and 18.

RP-1 Fuel System

The rocket-motor fuel system consisted of a pressurized fuel tank, filters, a flowmeter, a control valve, a cut-off valve, and associated tubing. A flow diagram of the fuel system appears in Figure 19.

The fuel, obtained from the supplier in 55-gallon drums, was transferred to the main fuel tank, which could hold 75 gallons. This tank could be pressurized to 1200 psi, however, the experiments required fuel pressures only as high as 800 psi. The tank was provided with an electrically-operated, fail-safe, vent valve and a burst diaphram.

With the fuel tank pressurized to the desired value, the fuel flow passed through a filter, a flowmeter, a control valve, a shut-off valve, and the injector of the rocket motor. The porous metal type of filter removed particles which might damage the flowmeter or the control valve, or might clog the small holes in the injector.

The flowmeter was of the impeller type. Rotation of the impeller was sensed by a magnetic detector. Output pulses from the digital sensor were transmitted to a converter which provided a suitable analog signal for recording on a pen-writing oscillograph. The converter also provided a means of setting the maximum flow rate (100 per cent value) and calibrating the flow system prior to an experiment. The calibrations were checked at intervals by flowing RP-1 through the flowmeter, collecting the liquid, and measuring the amount.

The flow rate of the fuel was determined by a throttle valve which was pneumatically actuated by a 3-15 psi signal pressure. As may be seen from Figure 19, the fuel line near the injector of the motor was so arranged that a manually-operated air purge could be used to remove residual fuel from the line prior to a run and after the experiment was completed. A manually-operated shut-off valve was provided to isolate the fuel system from the motor for calibrations and so forth.

Oxidizer System

The oxidizer used for these experiments was liquid oxygen. The LOX system was composed of a bulk LOX storage tank, an intermediate pressure tank, a porous metal filter, a flowmeter, a control valve, and associated stainless steel lines, regulators, and valves, as shown in Figure 20.

The bulk tank, installed for use on this project, held 300 gallons of LOX. The LOX was transferred from the bulk tank to the intermediate tank, a stainless steel pressure vessel (Fig. 21), held 50 gallons of LOX and could be filled from the bulk tank in about 30-40 minutes using pressures ranging from 75-125 psi in the bulk tank. A pneumatic fail-safe valve and a burst diaphram were utilized for protection too. The tank and line to the engine were well-insulated with polyurethane foam, using thicknesses of three inches and two inches, respectively.

Provision was made to evacuate the intermediate tank and line to the control valve to remove any moisture prior to filling the vessel with LOX. The porous metal filter was of the same type, but of different porosity, as that used in the fuel system. This filter removed particles which might have damaged the flowmeter or control valve, or have clogged the injector holes.

The flowmeter was of the impeller or "paddle-wheel" type, similar to the one used for the fuel system but having a different maximum range rating. Some difficulties were incurred during the early experiments because of the manufacturer's failure to remove the lubricant from the flowmeter which, consequently, became frozen and made the flowmeter inoperative during the experiment. The maximum capacity for the flowmeter was 2.25 pounds per second.

The control valve was similar to the one used in the fuel system. It was pneumatically operated and remotely controlled by a 3-15 psi signal pressure. This throttle valve, when not defrosted completely, which sometimes occurred when a number of tests were made in a short interval, had the tendency to become very sluggish or inoperative, causing loss of control of the LOX flow rate.

A regulated supply of gaseous oxygen was used to pressurize the intermediate tank containing the liquid oxygen. Tank pressures for these experiments ranged from 500 to 800 psi. All valves were pneumatic, remotely-controlled, fail-safe types. A purge was provided to clear the LOX lines before and after an experiment.

Coolant System

As with most previous rocket-motor experiments at this Laboratory, this rocket motor was cooled with high-pressure water. A coolant tank, having a 75-gallon capacity, was pressurized to values from 500 to 800 psi for these experiments. A burst diaphram and a fail-safe, pneumatically-operated vent valve were employed.

Coolant water was delivered through a porous metal filter, a turbine-type flowmeter, and an on-off solenoid valve to the rocket motor, as illustrated in Figure 22. Water entered the coolant jacket at the downstream end of the nozzle. By using a spiral groove, the water swirled around the external wall of the combustion chamber and exhaust nozzle and exited near the injector. The water was ejected into the air through a restriction which, in conjunction with the coolant tank pressure, determined the flow rate.

Coolant flow rates of approximately 1.5 pounds per second afforded satisfactory cooling for the copper combustion chamber - exhaust nozzle inserts. A thermocouple was inserted in the coolant flow at the point of exit from the coolant jacket to measure the water temperature.

The injector was connected to a separate cooling-water system, operated at normal water pressure, and consisted simply of a valve and lines to the injector.

Thrust Measurement

A thrust stand was constructed to hold the rocket motor in a vertical position with the exhaust jet pointed upward. This arrangement was necessary for these experiments in order to obtain a nearly interference-free field for the noise measurements. If the flame had pointed downward or at an angle, interference with the ground or other buildings or reflecting surfaces would have interferred with the measurements of the generated noise. By arranging the rocket motor in this position, the microphones were pointed toward the exhaust jet and did not receive significant contributions from reflecting surfaces.

The rocket motor was mounted on a pivoted plate on top of the thrust stand as shown in Figures 17 and 18. One end of the plate was pivoted and the other end rested on a hardened ball bearing embedded in a cantilevered beam. This triangular-shaped beam is shown in Figures 23 and 24 in detail. The reason for employing a cantilevered beam of this shape for thrust measurement is that the surface strain is uniform over the surface for loads applied at the tip. Thus, with strain gauges attached to the surface for thrust determination, the placement of the strain gauges was not critical.

Four strain gauges were employed, two on top and two on the bottom. These were arranged in a bridge circuit. Since negligible temperature gradients existed between the top and bottom sides of the plate, the strain gauges were temperature compensated. The strain-gauge bridge was excited with a carrier oscillator and the output then became a measure of the thrust. The entire system was calibrated by placing know dead weights on top of the rocket engine after all lines and

connections had been secured. Details of the bearing assembly for the thrust plate are shown in Figure 25. More details of the assembly are depicted in Figure 26.

All of these components were fabricated in the Laboratory machine shop. The frequency response of this strain gauge measuring system was quite adequate for the experiments performed. During the numerous experiments, there were a number of times that conditions developed wherein the motor oscillated rather strongly and the thrust measurement system detected these oscillations very nicely.

The thrust stand itself was placed outside the rocket pit which is used normally for rocket experiments. Physically the stand was positioned about five feet from the pit opening. During all of the experiments, the pit door was open along with the roof to have as few reflecting surfaces nearby as possible.

Noise Microphones

Four Kistler type 717A microphones were employed to detect the noise generated by the external jet of the rocket motor. They were placed at various distances and locations relative to the jet. The type 717A microphone consists of a type 701 quartz crystal pressure transducer and an electronic charge amplifier in a common housing. The charge amplifier is required to decouple the high impedance of the crystal transducer from the load connected to it. Basically, the crystal produces a charge that is proportional to the force on it. The output of the charge amplifier is a cathode follower which was employed to drive a low impedance coaxial cable to the instrumentation trailer. The output signal, power, and self-test connections to the charge amplifier were

made through a miniature four-pin connector. The entire microphone-amplifier housing is only 1.63 inches in length and the maximum diameter is 0.625 inch.

These microphones feature high sensitivity and a wide dynamic range. The maximum output signal is 5 volts. They have a very low acceleration sensitivity and a high overload capability. The basic specifications of this microphone are given in Table 1. Electrical power for the solid-state charge amplifier was provided by a 12-volt regulated power supply which was located in the instrumentation trailer. During the rocket-motor experiments, the output signals from the microphones were recorded on an Ampex instrumentation tape recorder having 7 channels and a 1/2-inch tape width, which met IRIG standards. When the tapes were replayed for analysis, the noise signals were displayed on a Singer model LP-1A audio spectrum analyzer.

When the system was calibrated for audio levels, every effort was made to simulate actual data acquisition conditions. Figure 27 illustrates the circuit employed. Each channel, including the microphone, tape deck, analyzer, and associated cables were calibrated as a unit to account for variation in the individual items, including the gain of the recorder amplifier.

An accurate audio self-test voltage was generated in the instrumentation trailer by using a precision audio signal generator. This voltage, transmitted to the microphones in position around the rocket motor, simulated the noise input to the microphone on the rocket stand. By introducing the measured, calibrating voltage at the microphone, a corresponding, simulated output signal of a specified number of

decibels was generated in accordance with the calibration provided by the manufacturer as illustrated in Figure 28. Calibration data are given in Table 2.

The output signals were recorded on the tape deck in the FM mode with a fixed gain on the individual recording channels. During playback, the trace on the spectrum analyzer was photographed thereby providing a permanent record of the analyzer deflection for a given db-level output from the microphones. Thus each individual system was calibrated from one end to the other. The self-test level required for an equivalent decibel simulation was determined from the microphone calibration data provided by the manufacturer for each microphone designated by serial numbers. The voltage and frequency of the self-test signal was adjusted accurately by using a digital frequency meter and an accurate audio voltmeter (VTVM) which gave RMS signal levels.

Each of the four microphone channels were checked at increments of 10 decibels from 110 db to 180 db, which was the operating range of the microphones. These measurements were made in 500-cycle increments from 4,000 cycles per second down to 500 cycles per second and in 20-cycle increments from 500 cycles per second to 20 cycles per second to verify the response of the entire system throughout the frequency range which was utilized in the experiments. The response over this dynamic range from 20 cycles per second to 4,000 cycles per second was flat. The tape deck, analyzer, and pen-writing oscillograph can be seen in Figure 29.

Rocket Firings

The physical characteristics of the rocket exhaust jet and the noise generated by it changed considerably as the mixture ratio of the propellant was changed. During many of the experiments, the mixture ratio was changed over a wide range during a single firing. As the mixture ratio was made quite rich, popping or explosive-like noises were heard with increasing frequency. Visually it was possible to see semi-periodic flashes of light which appeared to correlate well with the popping noises.

Figures 30-34 illustrate the firings at various stages during the experiments. The microphones can be seen on the four stands near the rocket motor.

SECTION IV

ANALYSIS OF EXPERIMENTAL RESULTS

The experimental data were analyzed in the following manner. First, a detailed examination was made of the oscillograph recording of the chamber pressure and propellant flow rates (mixture ratio). Next, various sections of the rocket engine experiment were selected on the basis of stability of all measurements during a fixed time interval. From the chart and a selection of the time intervals, the magnetic tape containing corresponding measurements of the intensity of the noise were then played back through the spectrum analyzer. At the appropriate time, an average value of the noise generated during this selected portion of the rocket engine run was obtained over a 10-second interval. Typical noise levels versus frequency spectra averaged over 10-second intervals

are shown in Figure 35. The corresponding chamber pressure and mixture ratio during the 10-second averaging interval also are shown. The measurements of the chamber pressure and mixture ratio were obtained from the oscillograph chart.

The frequency range indicated in Figure 35 was limited to the region below 4000 cps. This range was chosen since the main emphasis of this study was the generation of low-frequency noise. By comparison, the amount of noise above 4000 cps for this rocket motor is negligible.

During a given experiment with the rocket motor, we attempted to maintain a constant value of chamber pressure as the mixture ratio was varied. This procedure was followed in an attempt to maintain at a constant value that contribution to the noise level arising from the exhaust jet which is independent of chemical reactions. It is realized that simply maintaining the chamber pressure does not ensure an approximately constant exhaust velocity. In particular, the temperature also exerts a very pronounced influence on the exhaust velocity. From measurements of the noise at the higher frequencies we believe that we were able to maintain the non-combustion type noise at a fairly constant level. The photographs shown in Figure 35 indicate that the level of the noise at the low frequencies has a pronounced dependence on the mixture ratio. To a first approximation the noise level at the higher frequencies is independent of the mixture ratio.

In Figure 36 we have presented the average value of the noise level as a function of frequency for the spectra shown in Figure 35. In presenting the data we have employed a linear scale in frequency and have plotted the noise level at intervals of 250 cps from 250 cps to

3750 cps. Data from the other microphones obtained during the same time intervals are shown in Figures 37 and 38. The microphone for the data in Figure 36, was placed at the plane of the rocket exhaust nozzle, 21 inches from the thrust axis, while those in Figures 37 and 38 were 13 inches and 31.5 inches downstream and 34 inches and 37 inches to the side, respectively.

From a study of Figures 36 - 38, we find that, as we move further downstream, the effect of the fuel-rich mixtures on the noise level appears to be somewhat diminished. However, this may be an erroneous conclusion since the distance of the microphones from the exhaust jet was varied as well as the distance downstream. These effects could be clarified in future experiments. The important observations to be obtained from this set of data is the very pronounced effect of the mixture ratio on the magnitude of the low-frequency noise.

Figures 39 and 40 are typical data obtained from two other experiments in which measurements were made. Although the mixture ratio was varied from 1.60 to 3.03 (the stoichiometric mixture ratio is about 3.5), no noticeable intensification of the low-frequency noise was obtained. The principal purpose of these two figures is to indicate the accuracy of the data reduction methods. The fact that no intensification of low-frequency noise was obtained for the lowest mixture ratio of 1.6 places an upper limit on those mixture ratios which will produce intensification of the low-frequency noise level with the rocket motor employed in this study. Referring to Figures 36, 37, and 38, we find that the mixture ratios which produced noticeable intensification of the low-frequency noise were 1.40 and 1.17.

The results of the last experiment are shown in Figures 41 - 44. In this experiment, the microphones were mounted at the same radial distance from the exhaust jet (180 inches) and at distances of 0, 12, 24, and 48 inches downstream of the exhaust exit. The mixture ratio was varied from 0.92 to 3.70. In these figures the intensification of the low-frequency noise for rich mixture ratios is evident. The intensification for a mixture ratio of 0.92 is fairly pronounced while not as pronounced for a mixture ratio of 1.41. We believe that the effect of the mixture ratio of 1.41 is not as pronounced because the microphones were placed far away from the exhaust jet. The fact that the mixture ratio does not affect the intensity of the high-frequency noise is also indicated in the figures.

The results of these preliminary investigations revealed that the intensity of the low-frequency noise emitted by a small (250 - 500 lb thrust) rocket engine burning LOX and RP-1 may be considerably increased by burning fuel rich mixtures. Although the mixture ratio must be quite rich (less than 1.60) in the small rocket engine to achieve appreciable intensification of a low-frequency noise, we believe that the primary source of the low-frequency noise is the same for the small engines as for the large engines.

At this time we are unable to distinguish between the intensification of low-frequency noise due to combustion instability in the chamber, due to incomplete combustion in the chamber, or due to reactions between the exhaust gases and the atmospheric gases. One important aspect which must not be overlooked is the fact that the fuel-rich

mixtures do increase the intensity of the low-frequency noise which supports the explosion or detonation-wave theory of noise generation.

Although we have related the noise level to the mixture ratio in the present experiments, we believe that the noise emitted by larger engines will exhibit a stronger dependence on the mixture ratio, if the homogeneity of the mixture is less. It is important to note that the volume of the combustible mixture is greater for large engines than from small models. Hence, it is more likely that detonations may develop. For instance, in the present experiments employing a 250 - 500 lb thrust rocket engine, the mixture ratio must be less than 1.6 for appreciable intensification of the low-frequency noise. For a larger engine this "critical value" may be appreciably higher. In fact, for very large engines, very intense low-frequency noise may be generated for a stoichiometric mixture ratio or those near stoichiometric proportions by the combustion of pockets of unburned or incompletely burned fuel species reacting with the atmosphere.

SECTION V

CONCLUSIONS

We have shown that unburned fuel species which are present in the rocket exhaust jet, can react with the surrounding air to increase the intensity of low-frequency noise. We have not, to any great extent, been able to separate that portion of the noise due to the reactions with the atmosphere from the increased noise level due to the combustion process in the combustion chamber. It is extremely difficult at this time to distinguish between these two sources of noise. The

results reported herein are only preliminary results since a major part of the effort was devoted to the accurate recording of the noise signals and to obtaining data during reproducible experiments with the rocket motor.

We believe that more experiments should be undertaken to determine the basic mechanism of fuel-rich mixtures on the generation of low-frequency noise. From the experience obtained during this study, we feel that a fixed position of microphones plus a variation in nozzle divergence angle, mixture ratio, and combustion chamber size may produce a parametric study which would enable us to distinguish the combustion noise from the jet noise. Once these two sources of noise are distinguished, the next effort would be to employ different techniques to reduce the low-frequency noise due to combustion or detonation of the unreacted gases with the atmosphere. We anticipate that the reduction of the combustion-chamber noise would be a function primarily of the combustion-chamber design; however, this parameter has not been investigated very thoroughly. This parameter cannot be controlled, in general, because other factors ordinarily predominate in fabricating flight hardware. Therefore, the only source of noise which may possibly be reduced is the so-called external noise due to the reaction between the fuel species in the exhaust jet and the surrounding atmosphere.

REFERENCES

1. LIGHTHILL, M. J., "On Sound Generated Aerodynamically. I. General Theory," Proc. Roy. Soc. A., Vol. 211, pp 564-587, 1952.

2. LIGHTHILL, M. J., "On Sound Generated Aerodynamically. II. Turbulence as a Source of Sound," Proc. Roy. Soc. A., Vol. 222, pp 1-32, 1954.

3. FJOWCS WILLIAMS, J.E., "The Noise from Turbulence Convected at High Speed," Phil. Trans. Roy. Soc. London, 255, pp 469-503, 1963.

4. RIBNER, H. S., Advances in Applied Mechanics, Vol. 8, Academic Press, New York, 1964.

5. LIGHTHILL, M. J., "Sound Generated Aerodynamically," Proc. Roy. Soc. A., Vol. 267, pp 147-182, 1962.

6. MORGAN, W. V., SUTHERLAND, L. C. and YOUNG, K. J., "The Use of Acoustic Scale Models for Investigating Near Field Noise of Jet and Rocket Engines," Flight Dynamics Laboratory, WADD Technical Report 61-178, Wright-Patterson Air Force Base, Ohio, April 1961.

7. COLE, J. N., et al., "Noise Radiation from Fourteen Types of Rockets in the 1,000 to 130,000 Pounds Thrust Range," WADC Technical Report 57-354, Wright Air Development Center, Wright-Patterson Air Force Base, Ohio, December 1957.

8. POWELL, A., "On the Generation of Noise by Turbulent Jets," ASME Paper 59-AV-53, 1959.

9. ROLLIN, V. G., "Effect of Jet Temperature on Jet-Noise Generation," NACA TN 4217, 1958.

10. RIBNER, H. S., "Energy Flux from an Acoustic Source Contained in a Moving Fluid Element and Its Relation to Jet Noise," J. Acoust. Soc. Am., Vol. 32, September 1960.

11. POWELL, A. and SMITH, T. J. B., "An Aerosonics Bibliography," University of California, Los Angeles, Report No. 63-51, October 1963.

12. ELDRED, K., ROBERTS, W., et al., "Structural Vibration in Space Vehicles. Phase I Report. Investigation of Structural Vibration Sources and Characteristics," NOR-60-26 Progress Report of the Dynamics Branch, Northrop Corp. and Western Electro-Acoustic Laboratories, January 1960.

13. ESCHENROEDER, A. Q., "Intensification of Turbulence by Chemical Heat Release," Physics of Fluids, Vol. 7, No. 11, pp 1735-1742, November 1964.

TABLE I

General Microphone Specifications

Fundamental range	+180 db*
Threshold	+100 db*
Fundamental range (pressure)	3 psi (rms)
Over-range capacity	30 psi (max)
Output level (nominal)	5 volts peak-to-peak
Sensitivity (nominal)	0.5 volts/psi
Linearity	±1% of calibrated range
Natural frequency	60,000 cycles/second
Frequency response (± 5% (1 Meg. load))	6-15,000 cycles/second
(± 30% (1 Meg. load))	2-25,000 cycles/second
Rise time	8 milliseconds
Time constant	0.1 second
Output impedance	100 ohms
Acceleration sensitivity	0.02 psi/g
Temperature sensitivity	0.01%/°F
Temperature range	-65 to +180°F
Intermittent gas temperature	3,000°F
Shock	1,000 g for 1 millisecond
Vibration	100 g (5-2000 cycles/second)
Weight	50 grams

*Referred to 2×10^{-4} dynes/cm^2 (2.96×10^{-9} psi (rms))

TABLE 2

Microphone and Charge Amplifier Characteristics

	Serial No. of Microphone and Amplifier			
	112	113	114	115
Microphone Sensitivity (pCb/psi)	5.8	5.8	5.8	5.8
Charge Amplifier Sensitivity (mv/pCb)	99.1	103.0	93.0	104.5
Self-Test Sensitivity (pCb/volt)	10.5	10.6	10.7	11.9
Assembly Sensitivity (volt/psi)	0.575	0.591	0.534	0.600
+120 db Point Measured at 400 cycles/second (mv-rms)	1.64	1.73	1.54	1.76

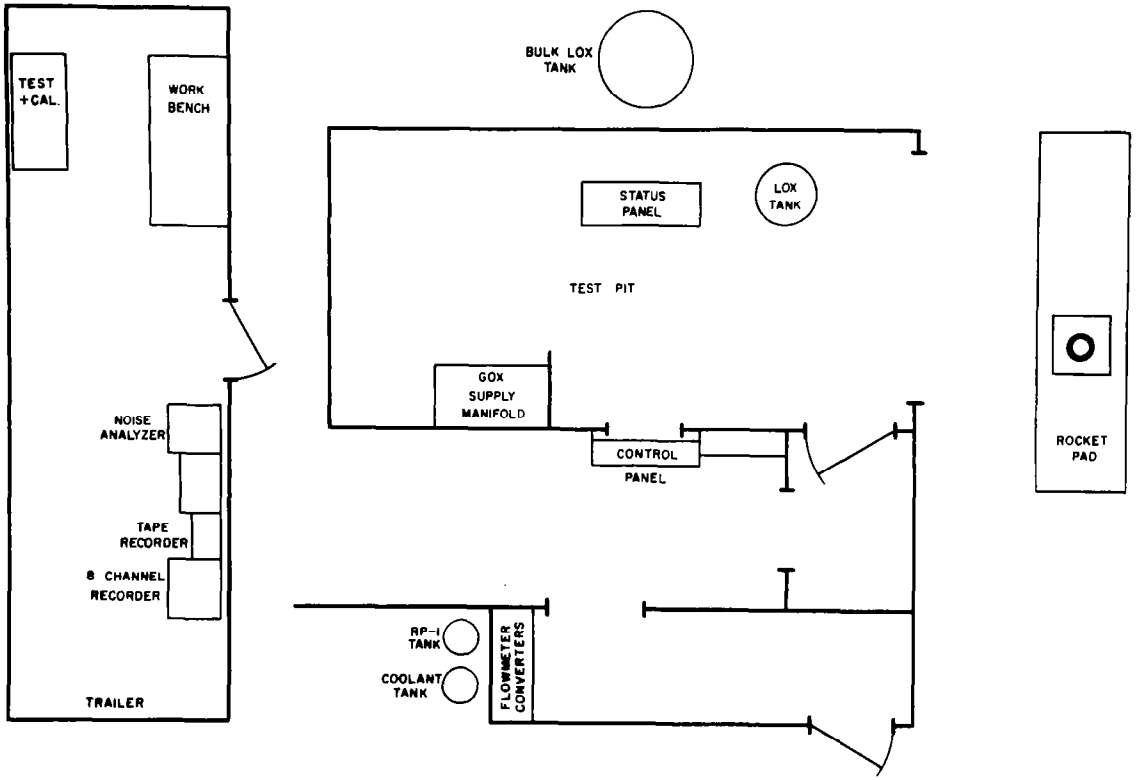

Figure 1 - Experimental Facilities

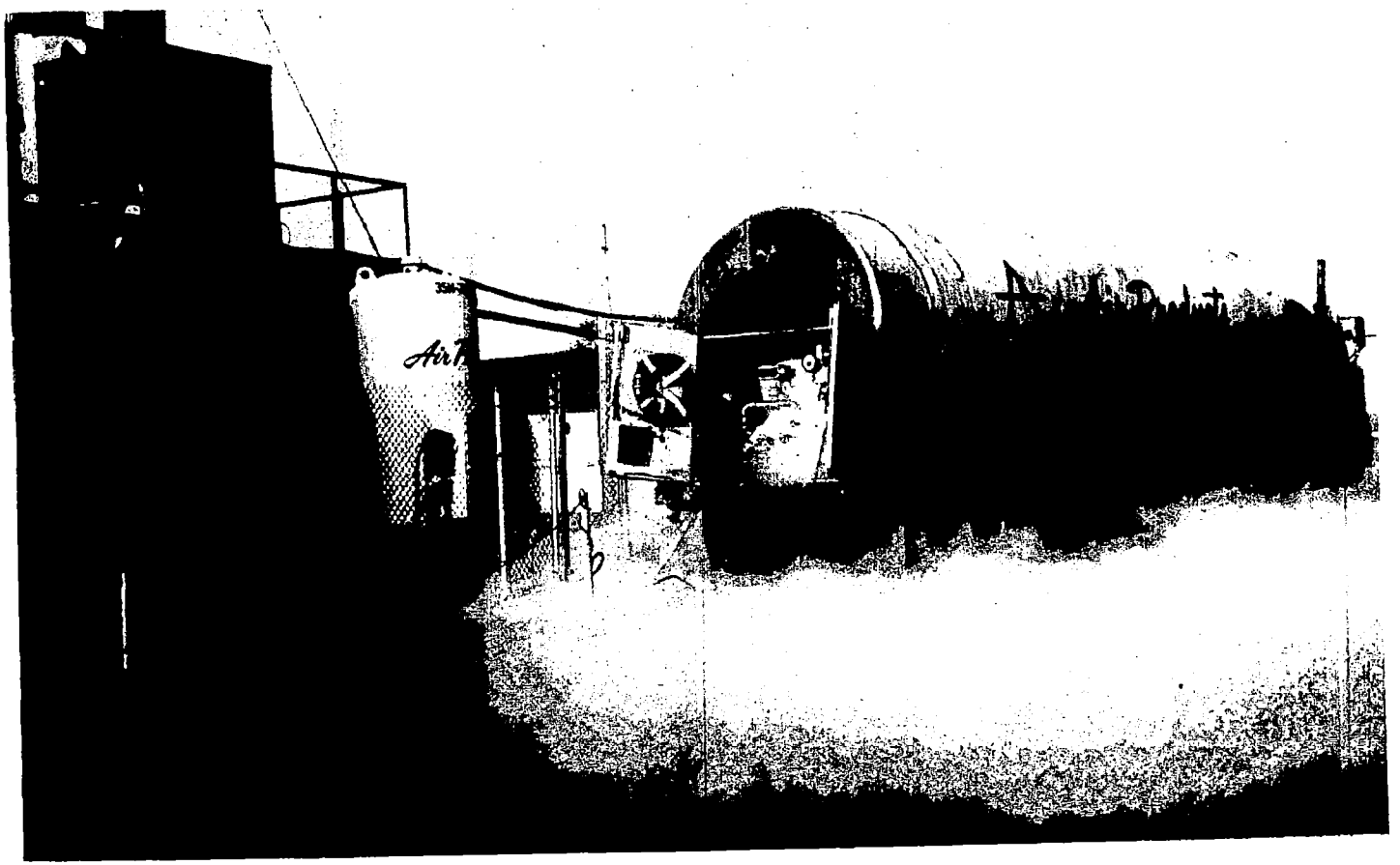

Figure 2 - Delivery of Liquid Oxygen to Supply Tank

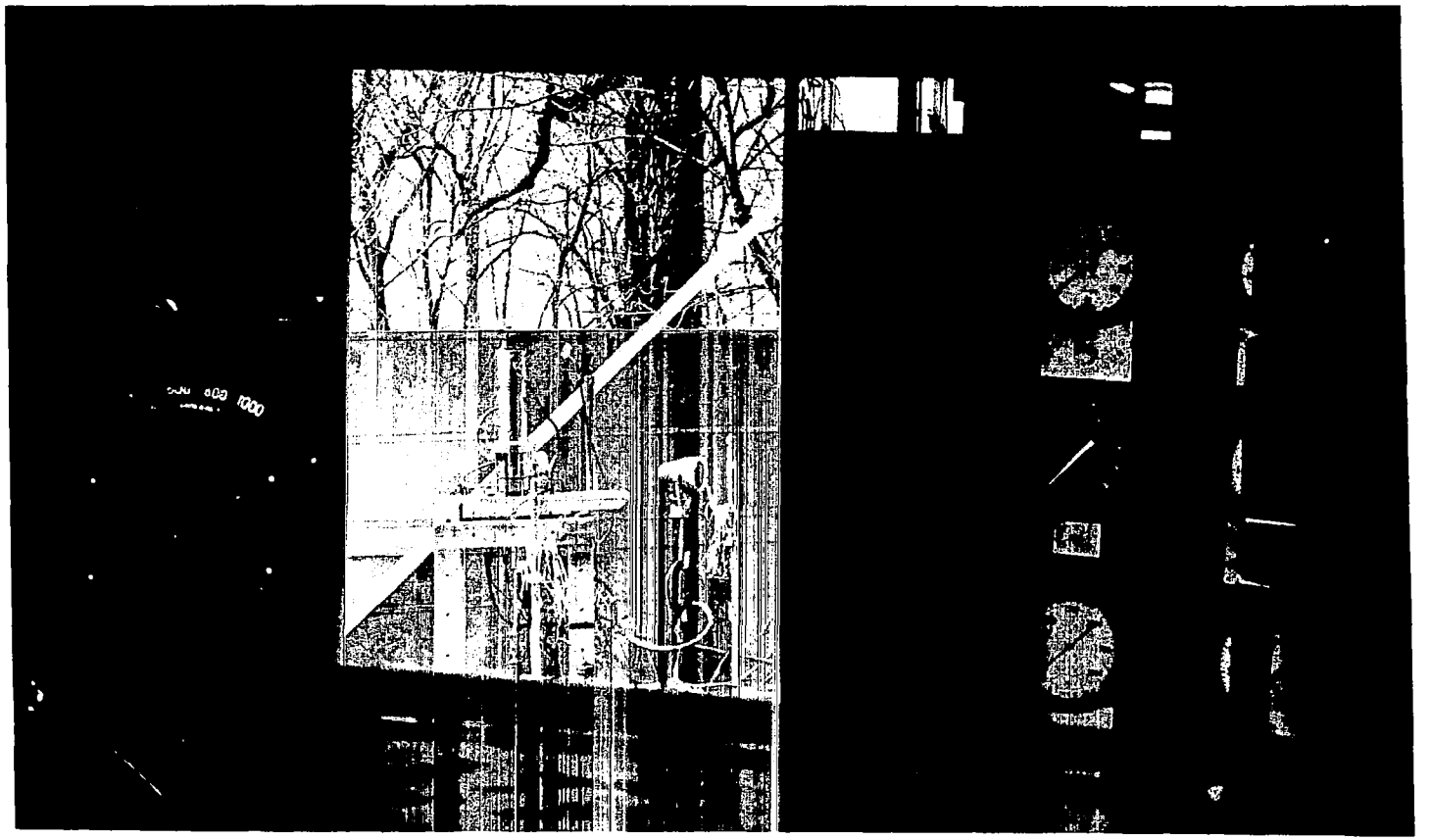

Figure 3 - View of Rocket Motor from Control Panel

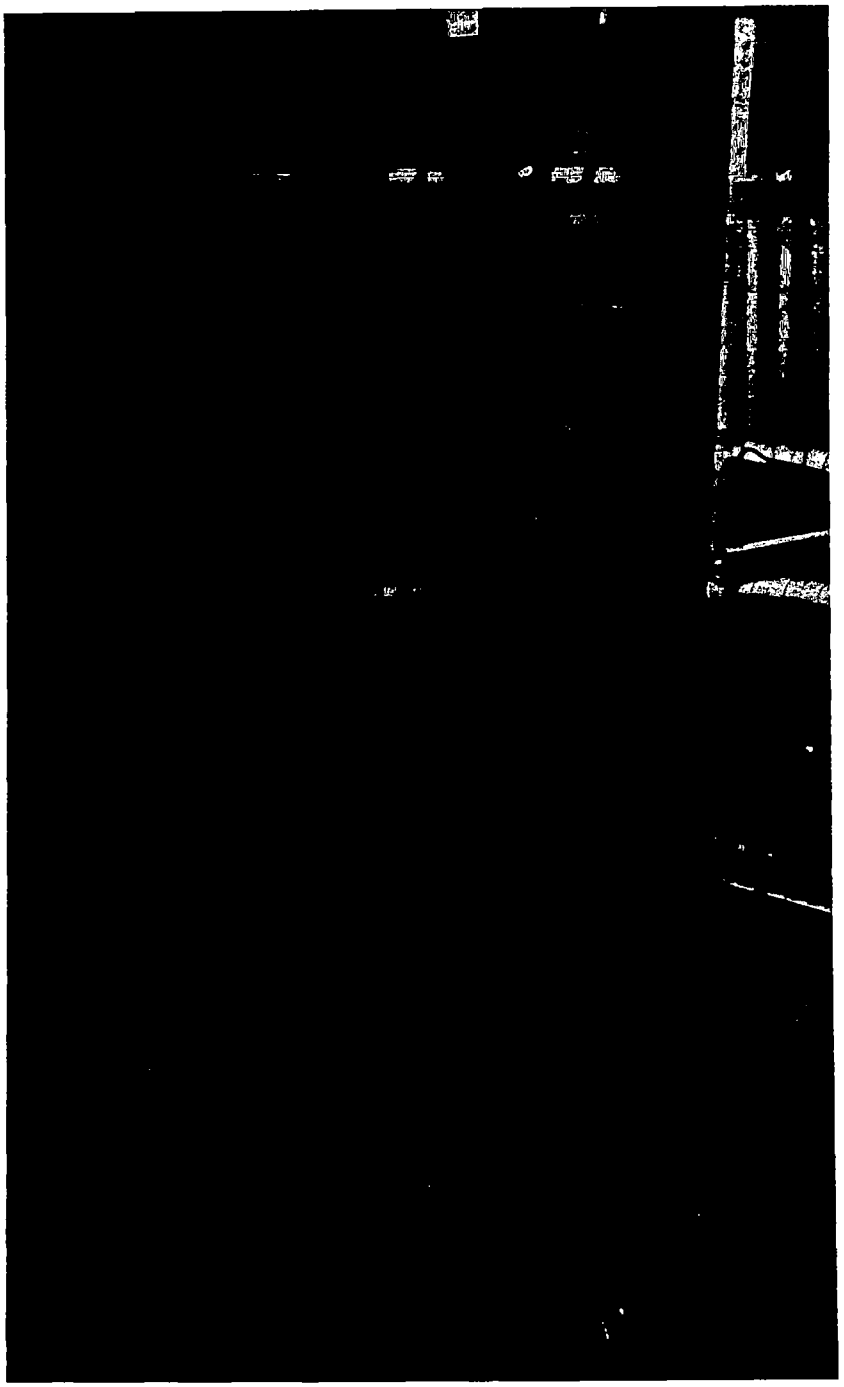

Figure 4 - Gauge Panel Used by Operator During an Experiment

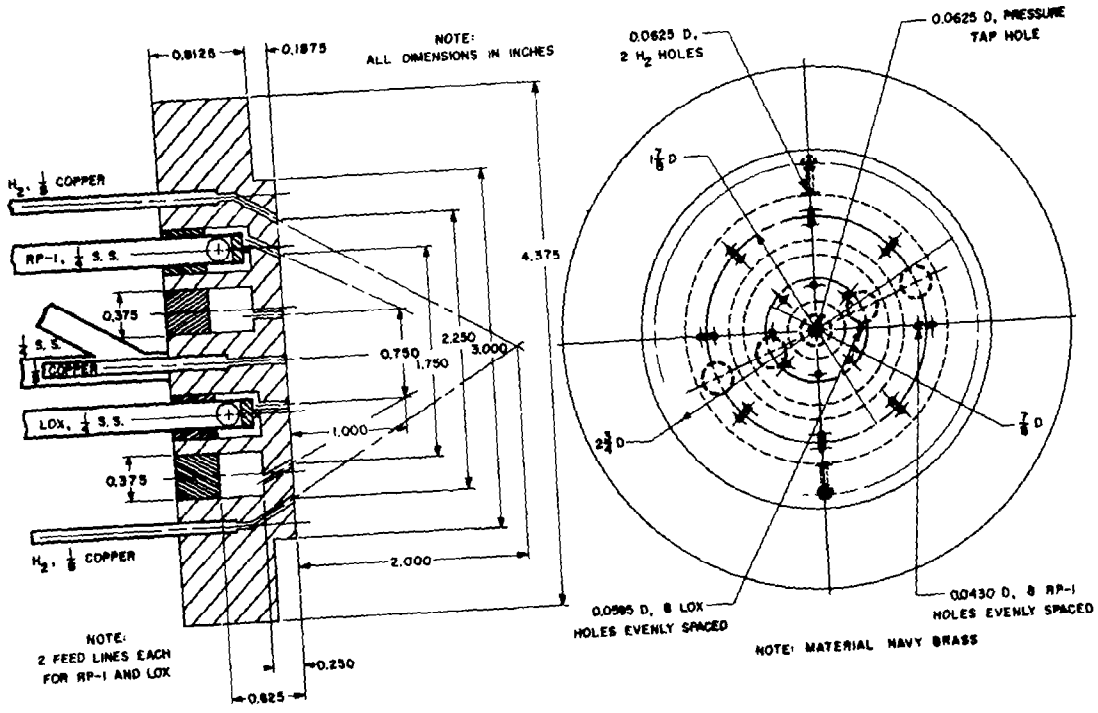

Figure 5 - Rocket Injector A-1

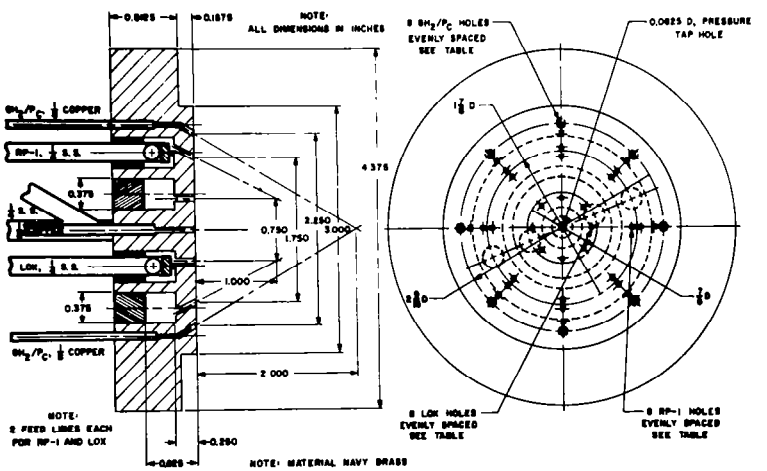

INJECTOR NO.	LOX HOLE DIA.	RP-1 HOLE DIA.	GH_2/P_C HOLE DIA.
1A-1	0.059	0.043	0.0625
1A-2	0.076	0.056	0.0625

Figure 6 - Rocket Injector 1A-1, 1A-2

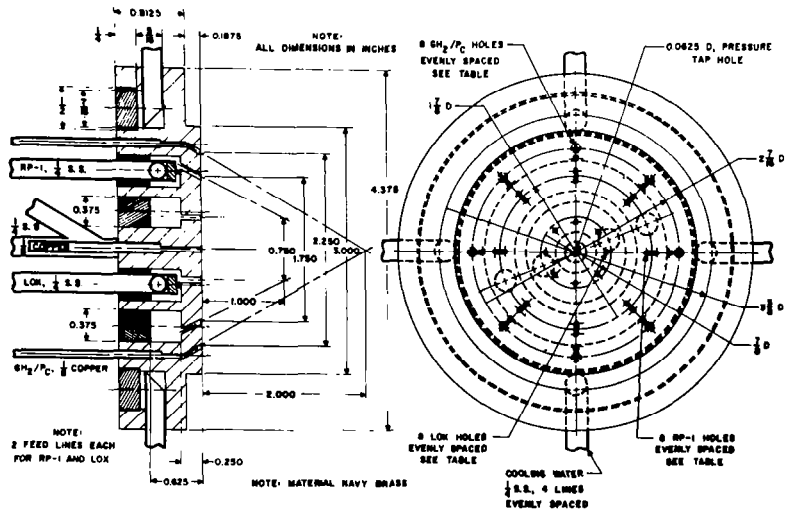

INJECTOR NO.	LOX HOLE DIA.	RP-1 HOLE DIA.	GH_2/P_C HOLE DIA.
1A-3	0.093	0.070	0.0625
1B-1	0.093	0.070	0.0625

Figure 7 - Rocket Injector 1A-3, 1B-1

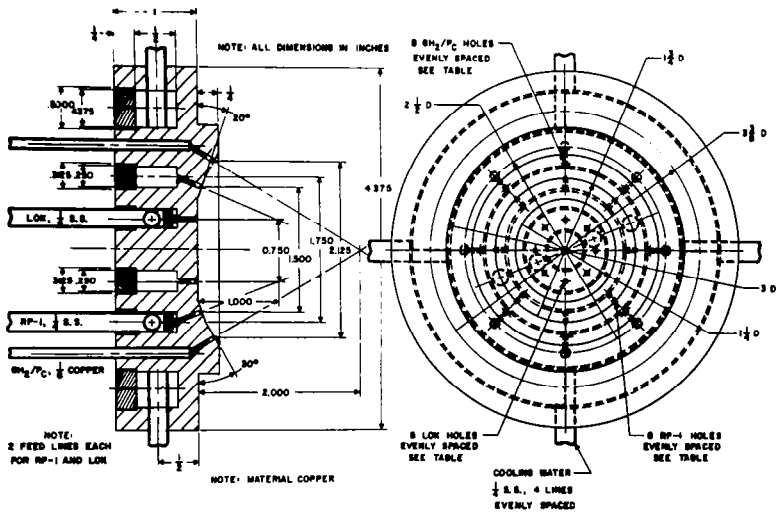

INJECTOR NO.	LOX HOLE DIA.	RP-1 HOLE DIA.	OH_2/P_C HOLE DIA.
IC-1	0.0937	0.070	0.0625

Figure 8 - Rocket Injector 1C-1

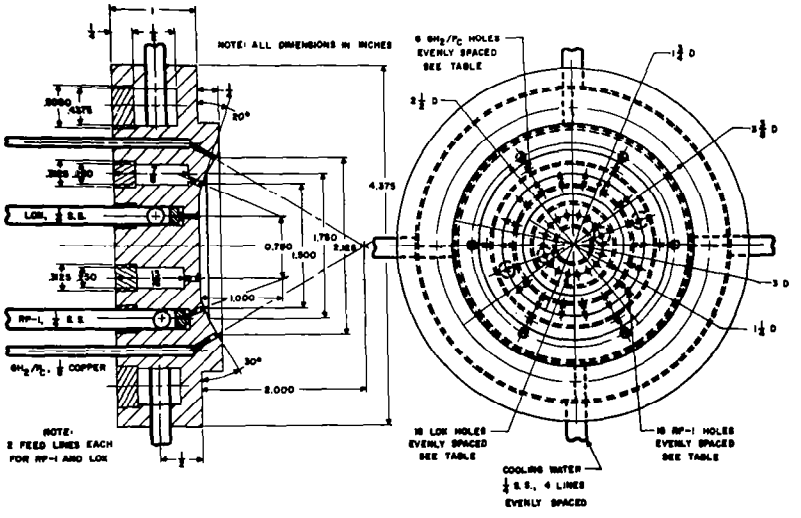

INJECTOR NO.	LOX HOLE DIA.	RP-1 HOLE DIA.	GH_2/P_C HOLE DIA.	MATERIAL
1D-1	0.018	0.022	0.0625	BRASS

Figure 9 - Rocket Injector 1D-1

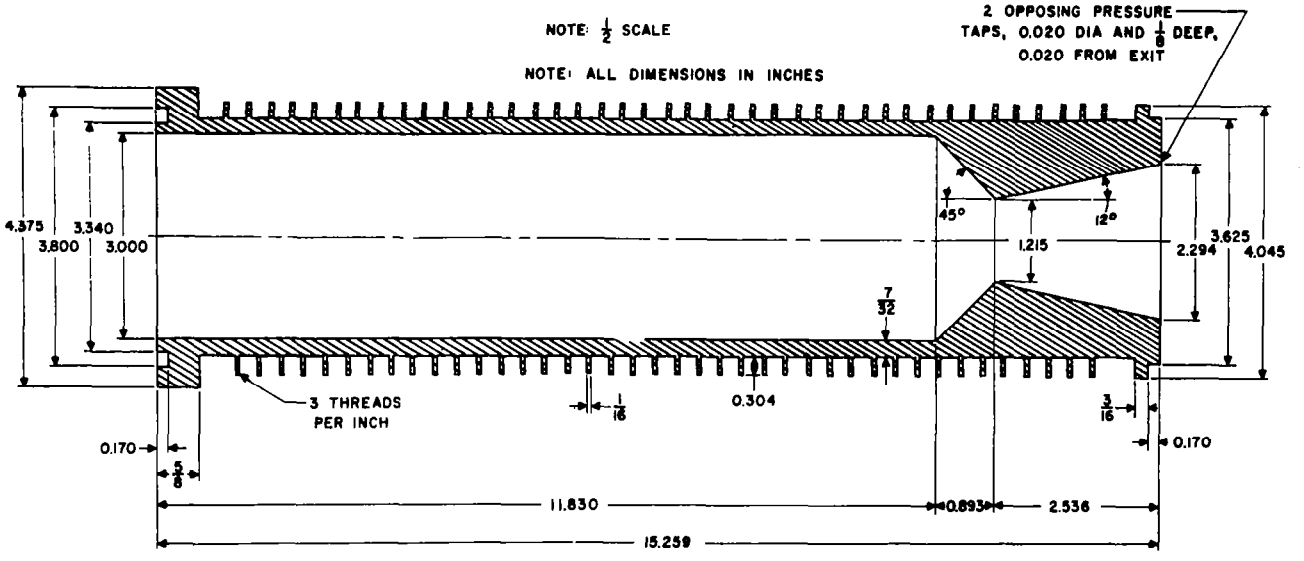

Figure 10 - Combustion Chamber Insert, 500 - Pound Thrust Nozzle

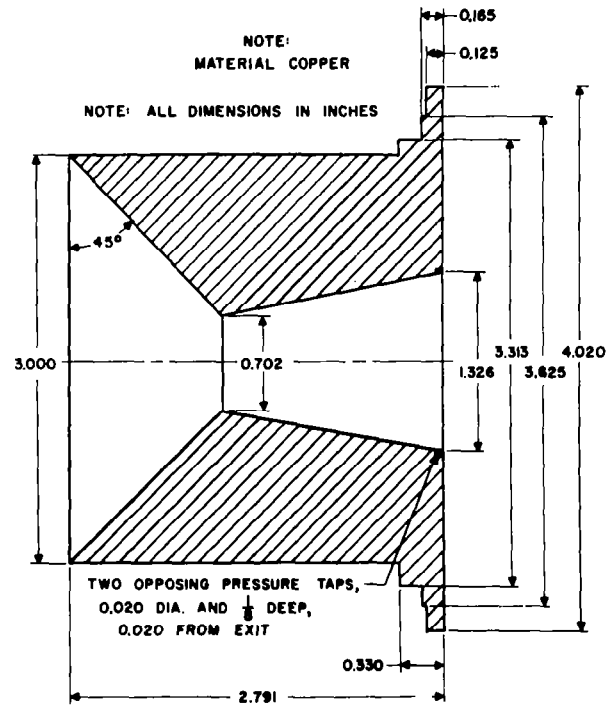

Figure 11 - 175 - Pound Thrust Nozzle Insert

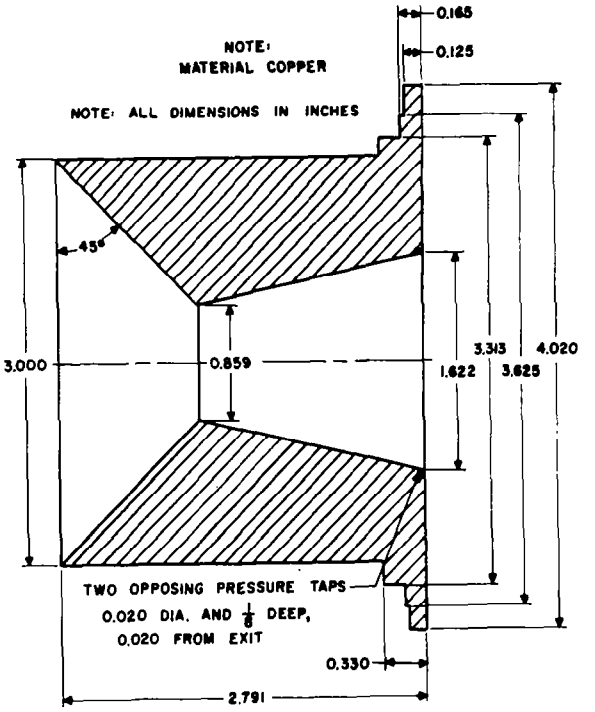

Figure 12 - 250 - Pound Thrust Nozzle Insert

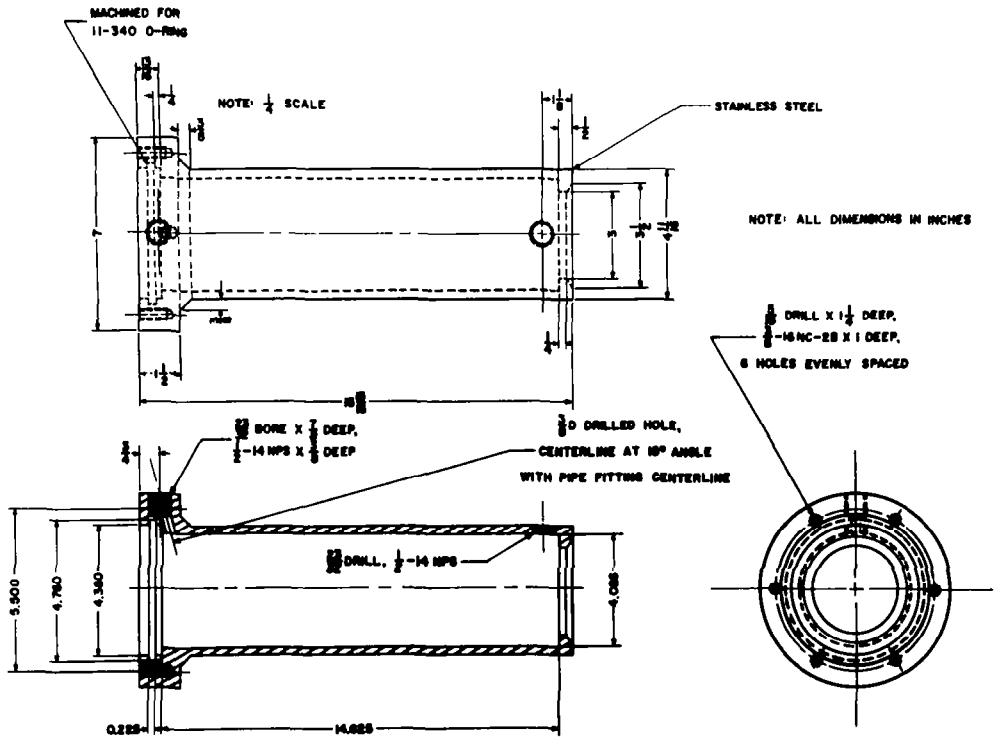

Figure 13 - Rocket Engine Coolant Jacket Model 1

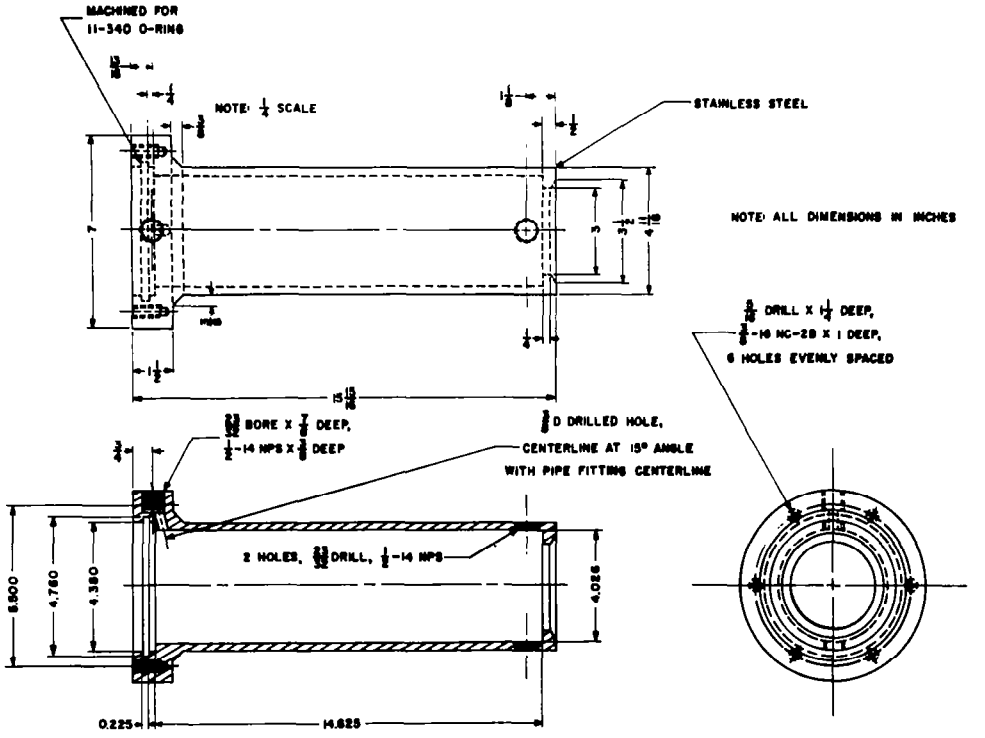

Figure 14 - Rocket Engine Coolant Jacket Model 2

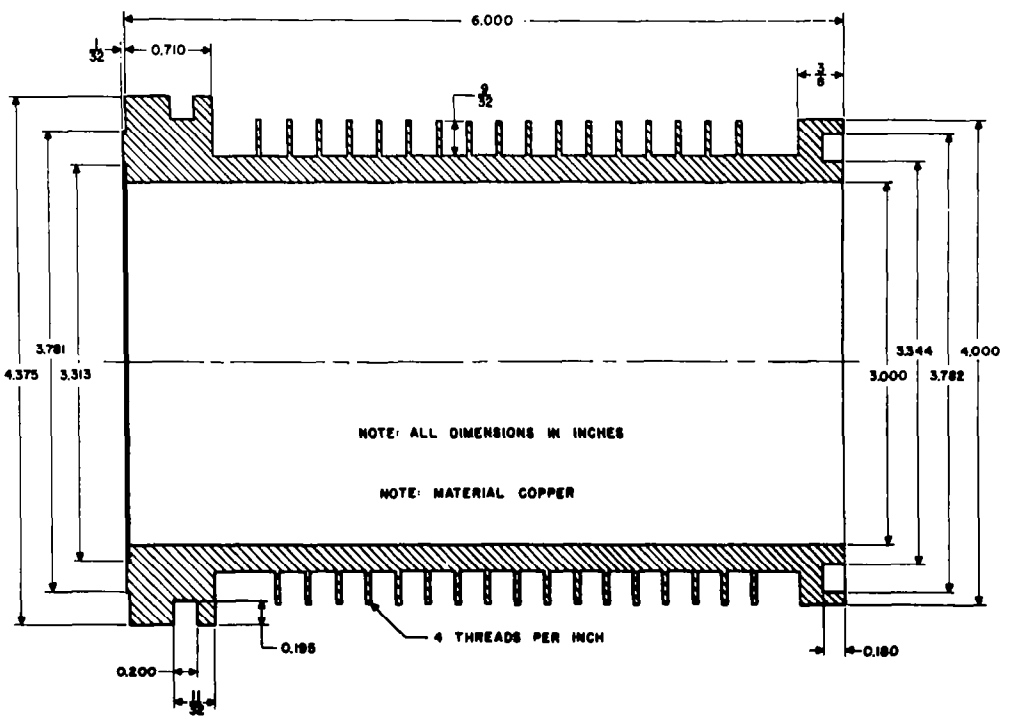

Figure 15 - Combustion Chamber Extension

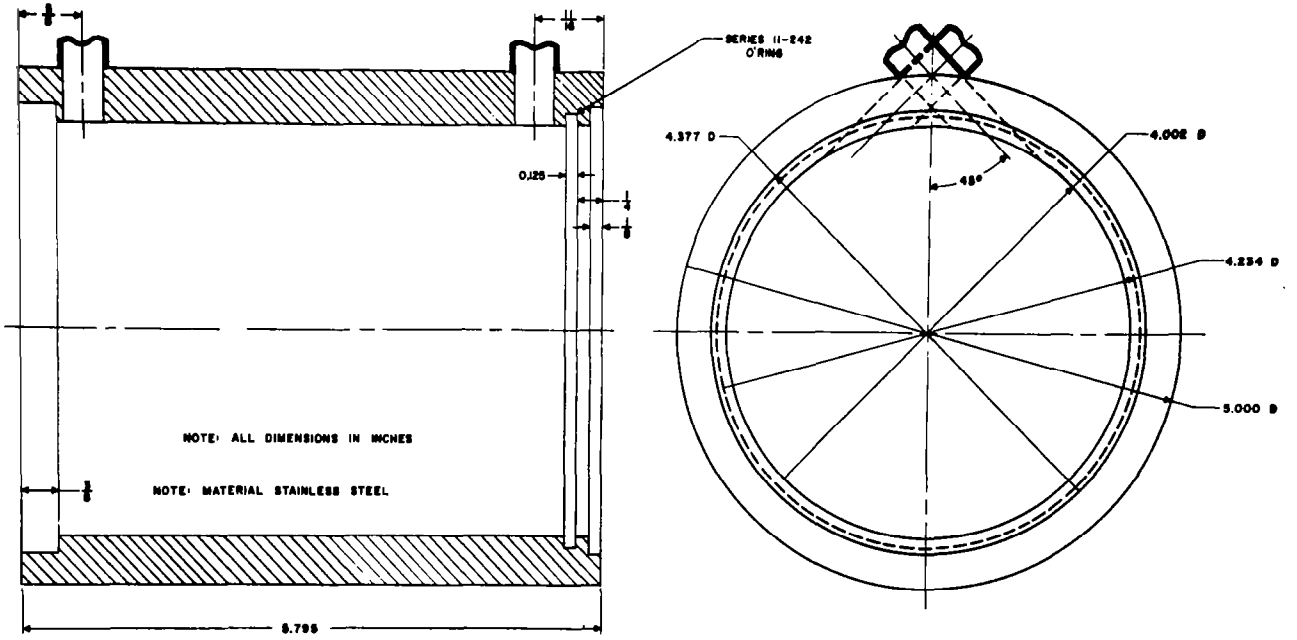

Figure 16 - Rocket Engine Extension Coolant Jacket

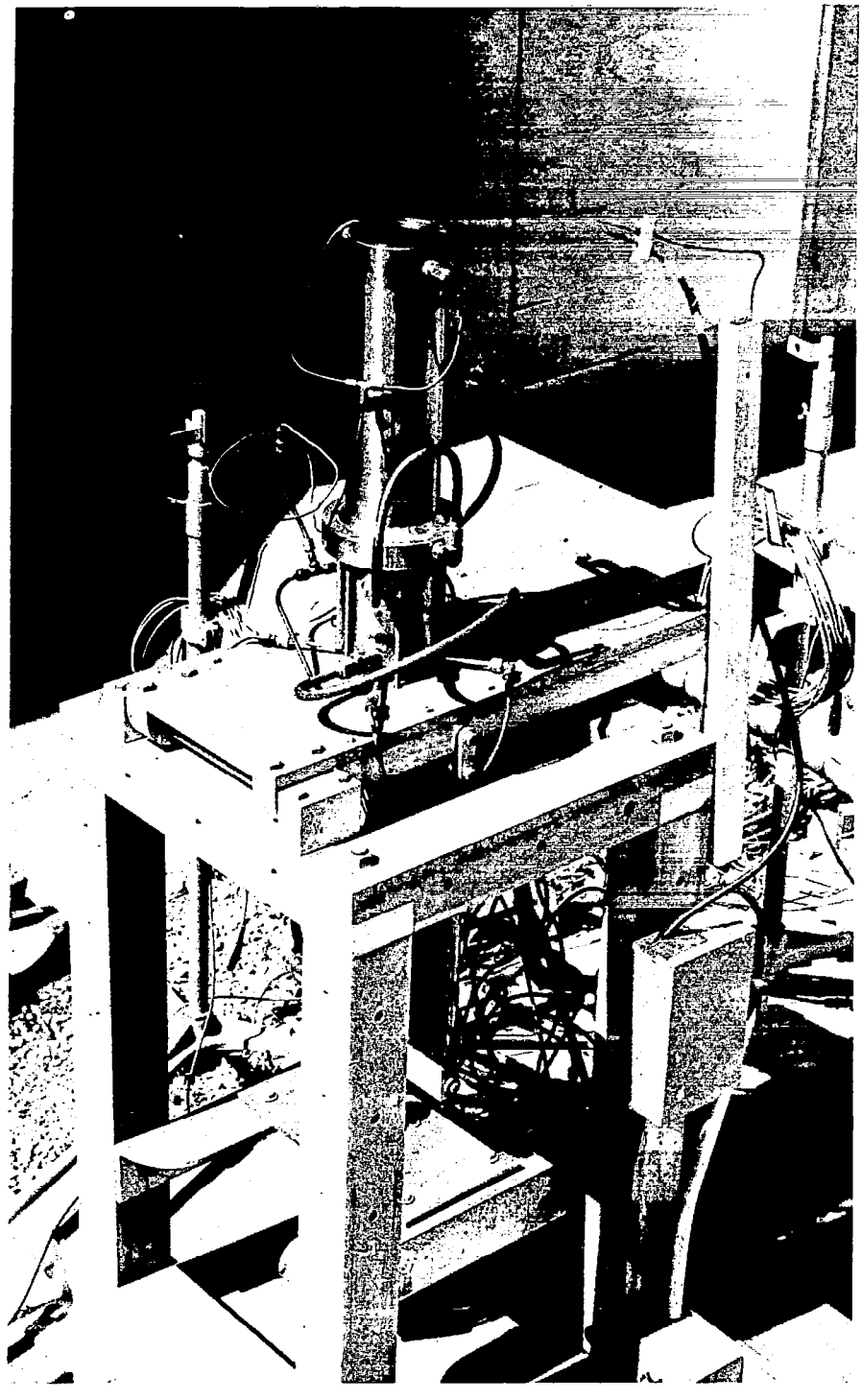

Figure 17 - Side View of Rocket Engine on Thrust Stand

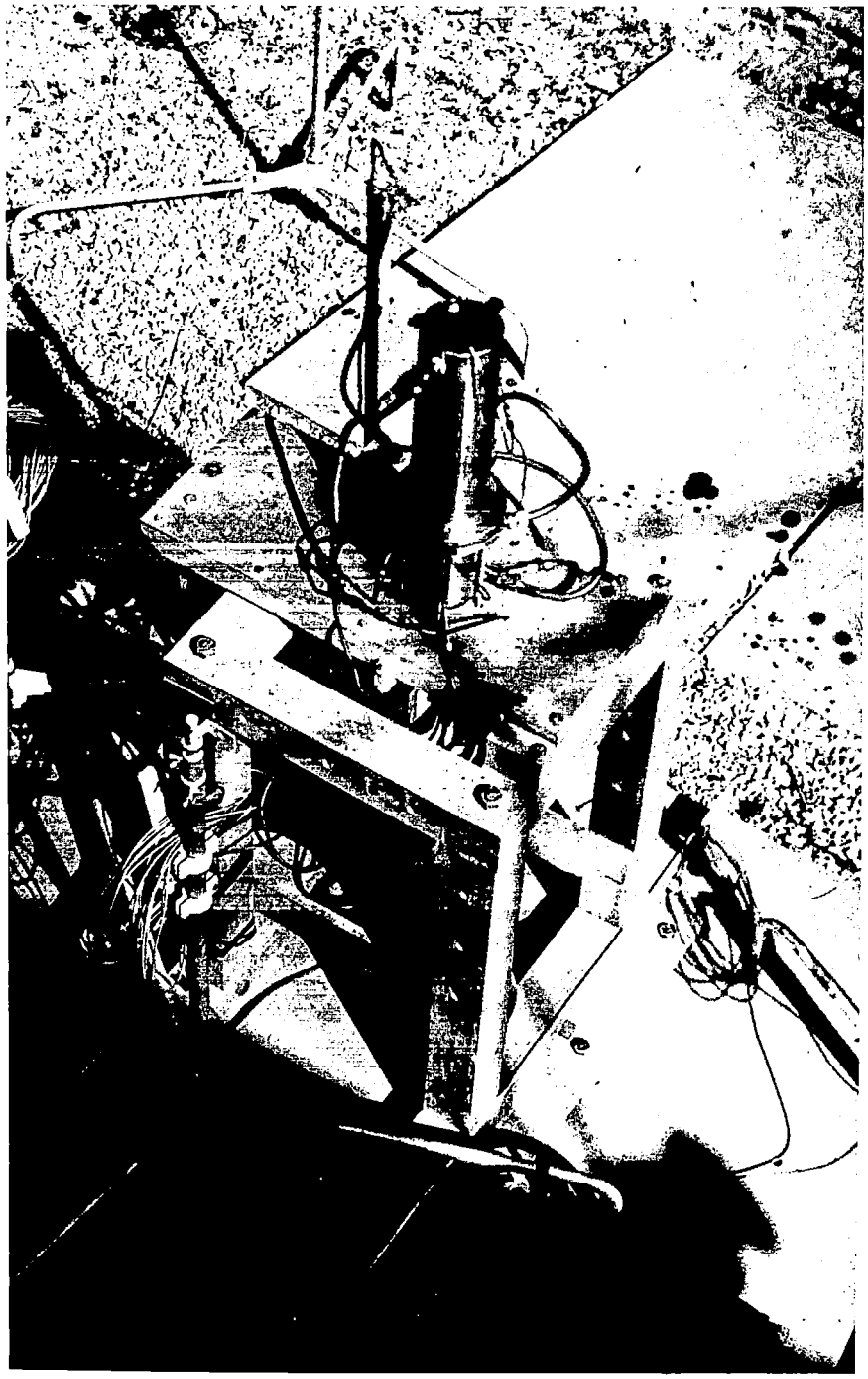

Figure 18 - Top View of Rocket Engine on Thrust Stand

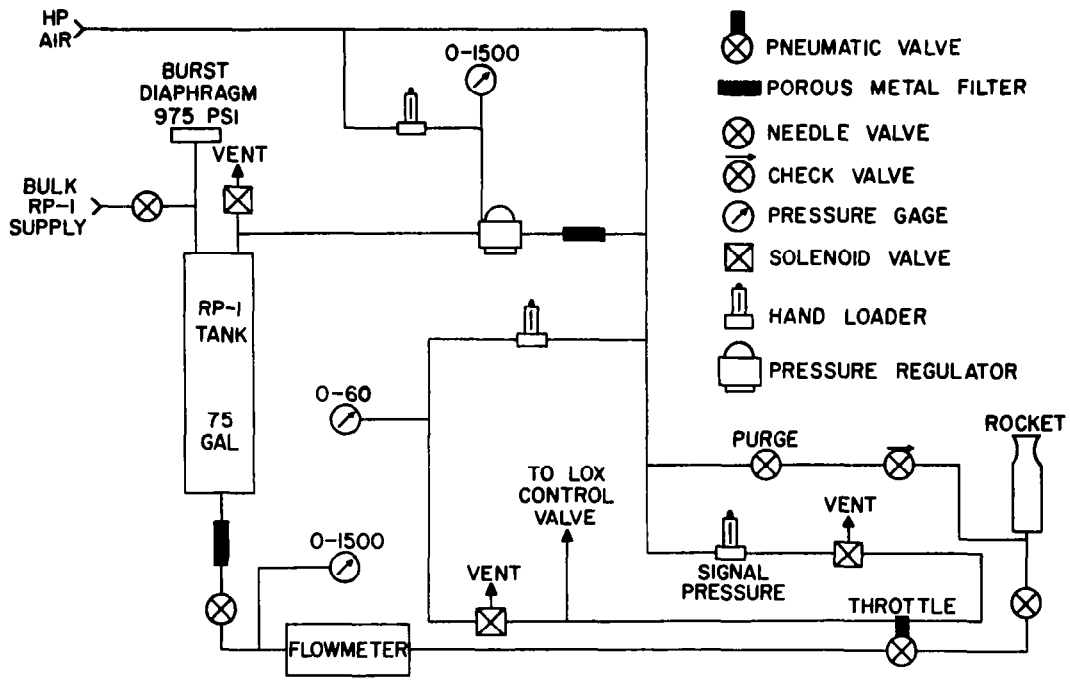

Figure 19 - Rocket Engine Fuel System

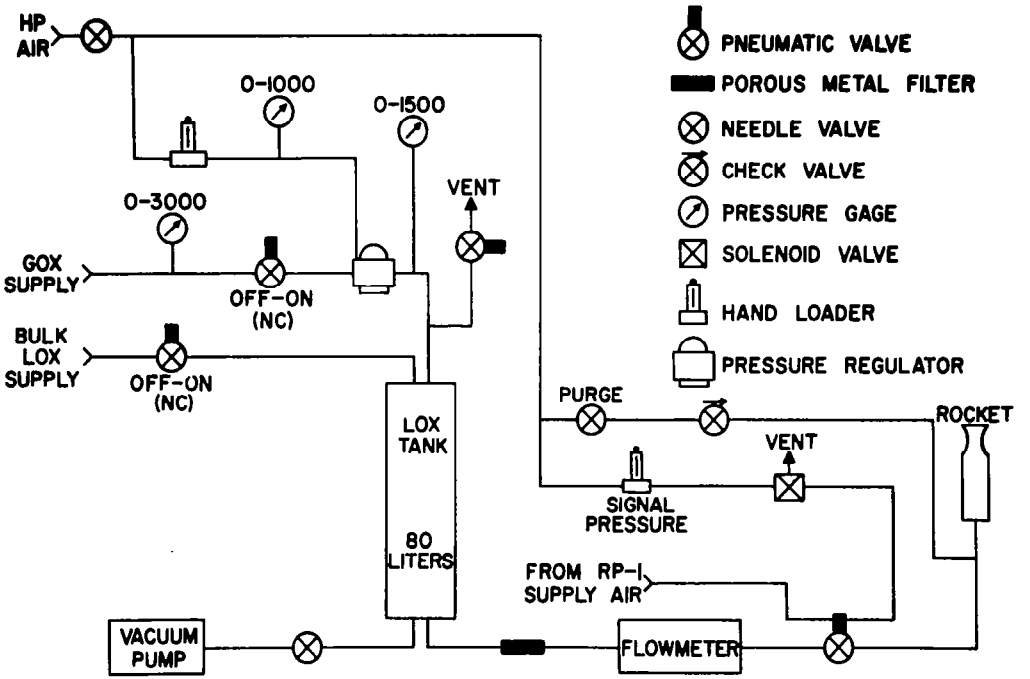

Figure 20 - Rocket Engine Oxidizer System

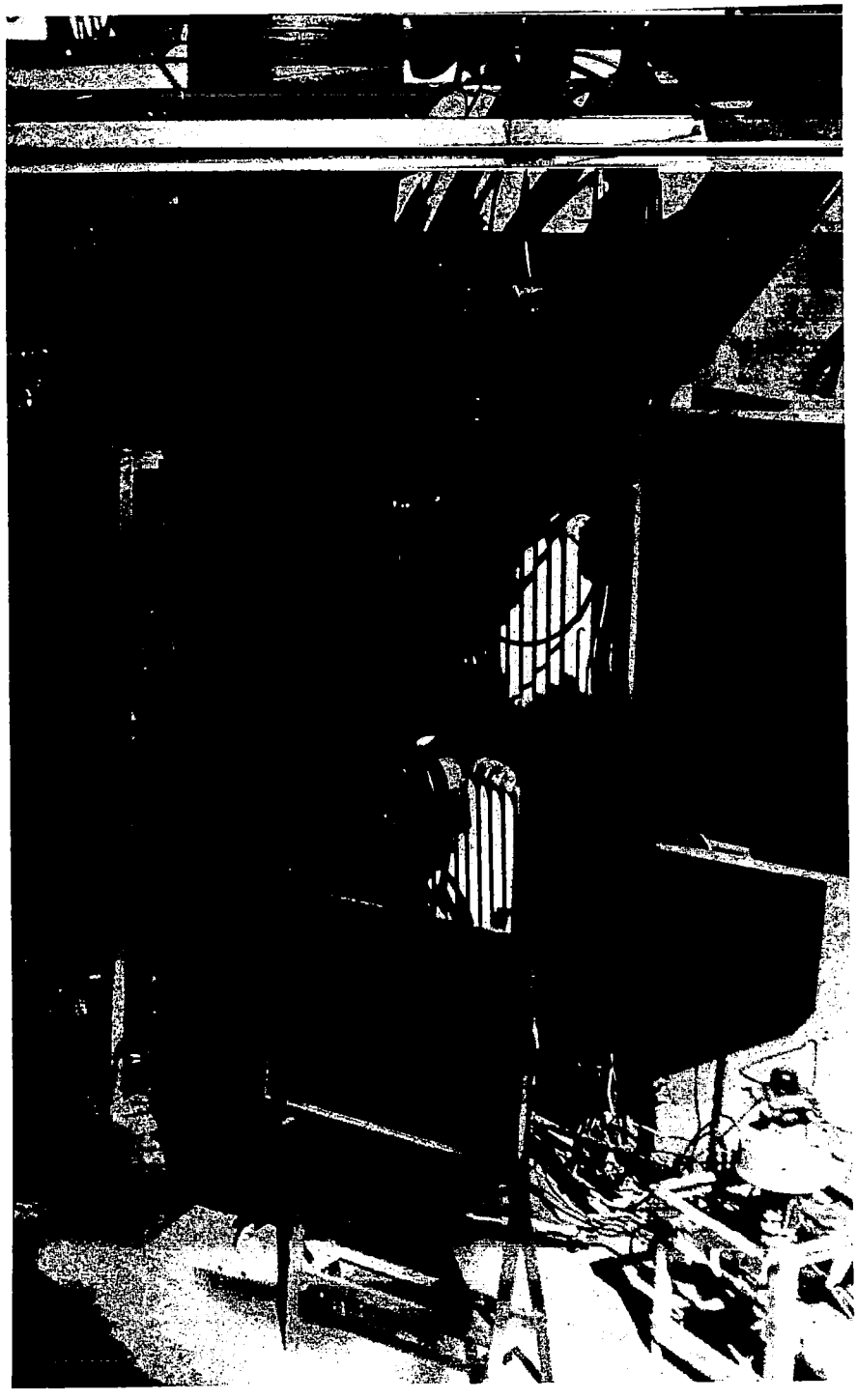

Figure 21 - Liquid Oxygen Pressure Vessel and Flow Control Valve

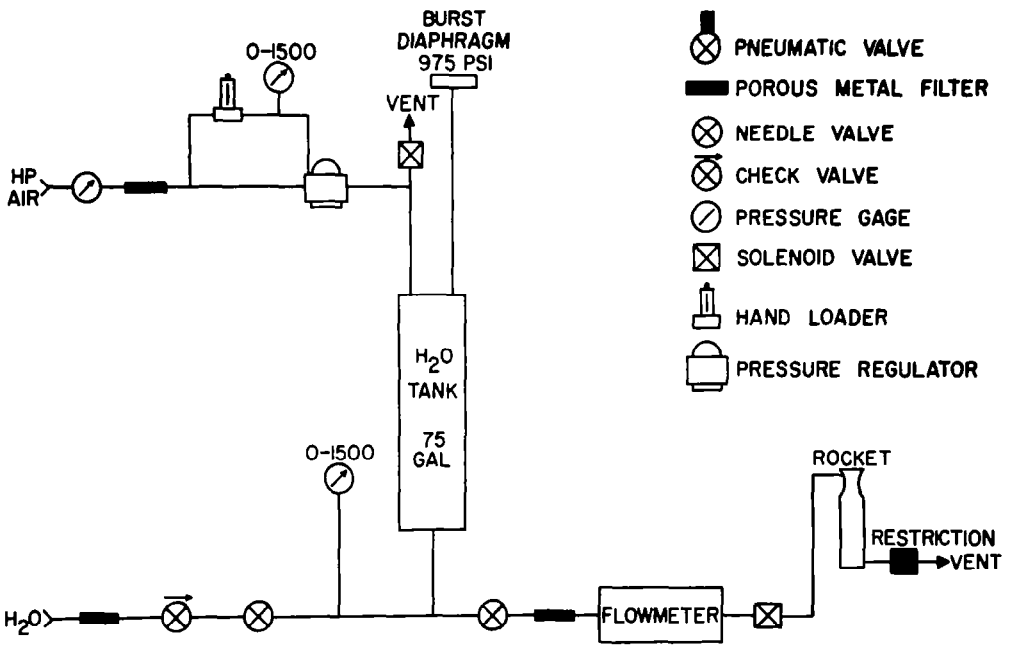

Figure 22 - Rocket Engine Coolant System

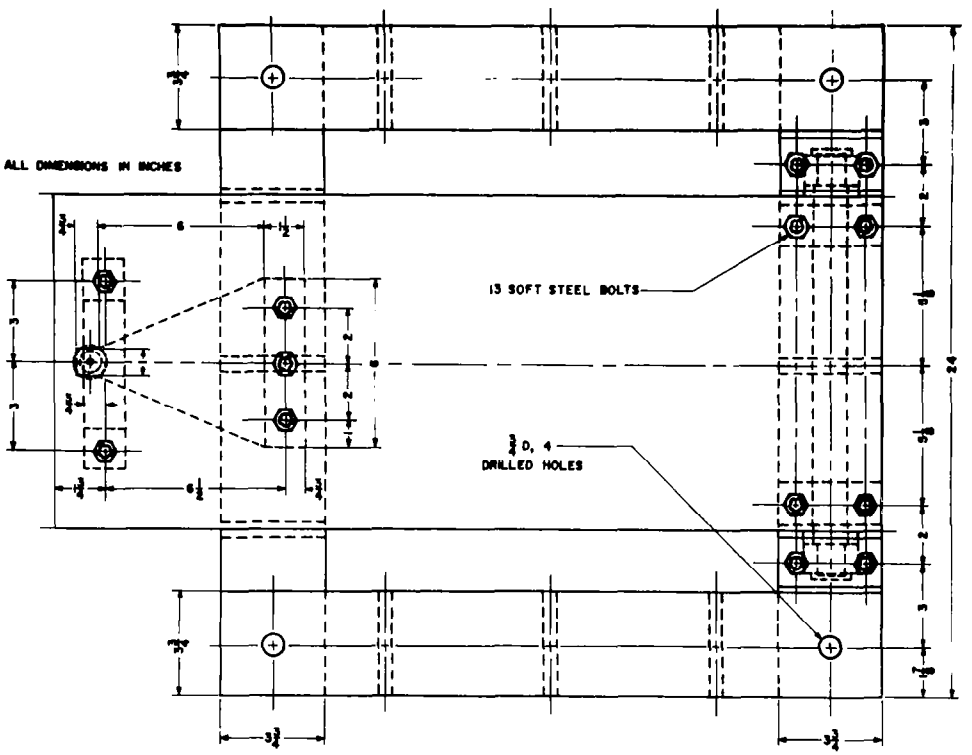

Figure 23 - Top View of Engine Mounting Plate Assembly

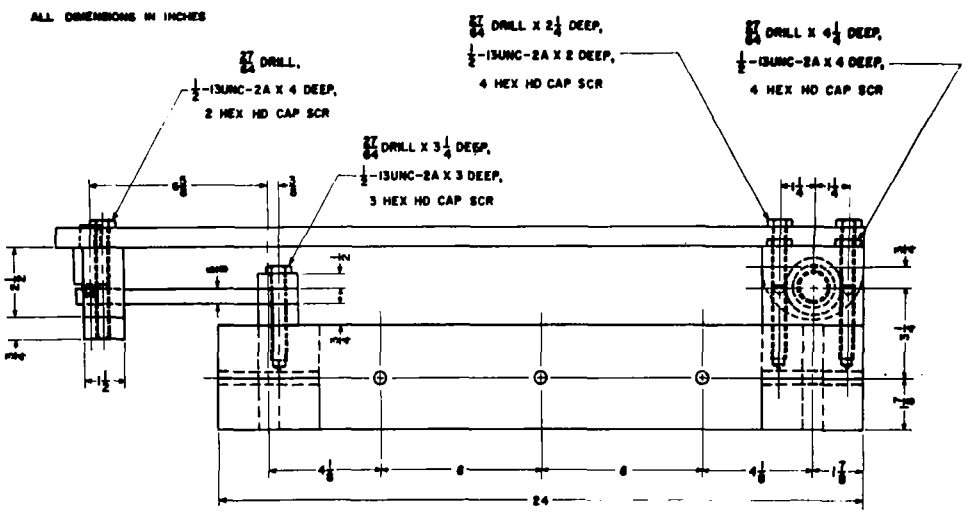

Figure 24 - Front View of Engine Mounting Plate Assembly

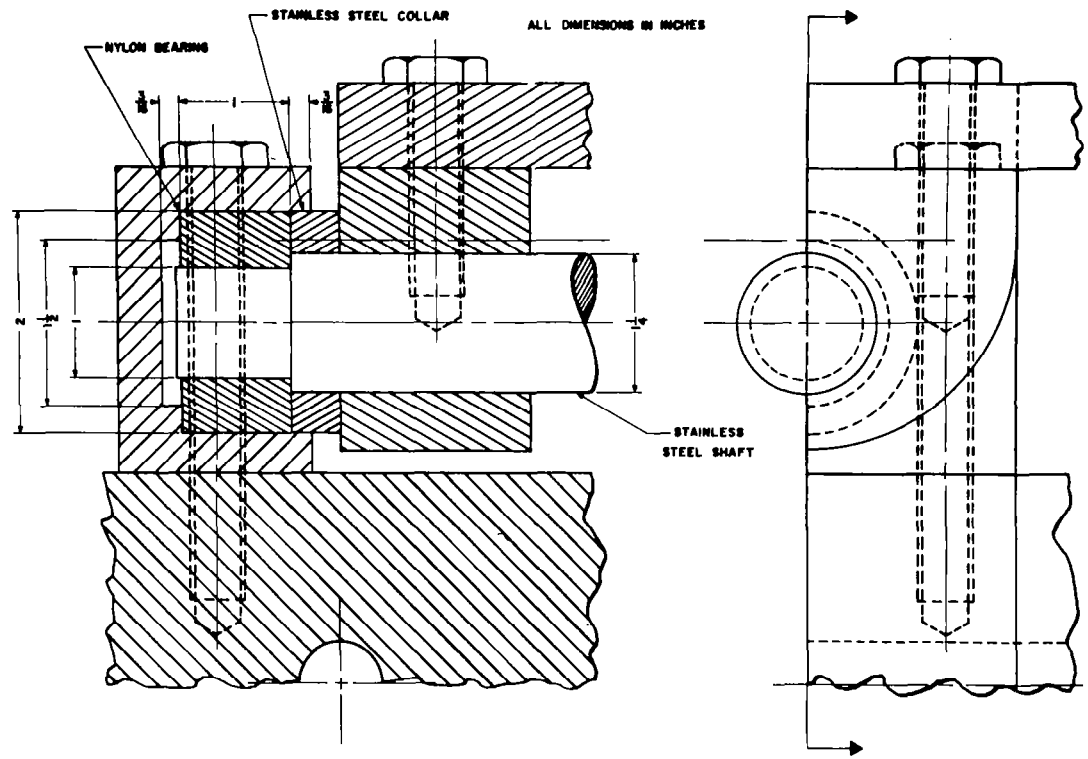

Figure 25 - Sectional View of Bearing Assembly

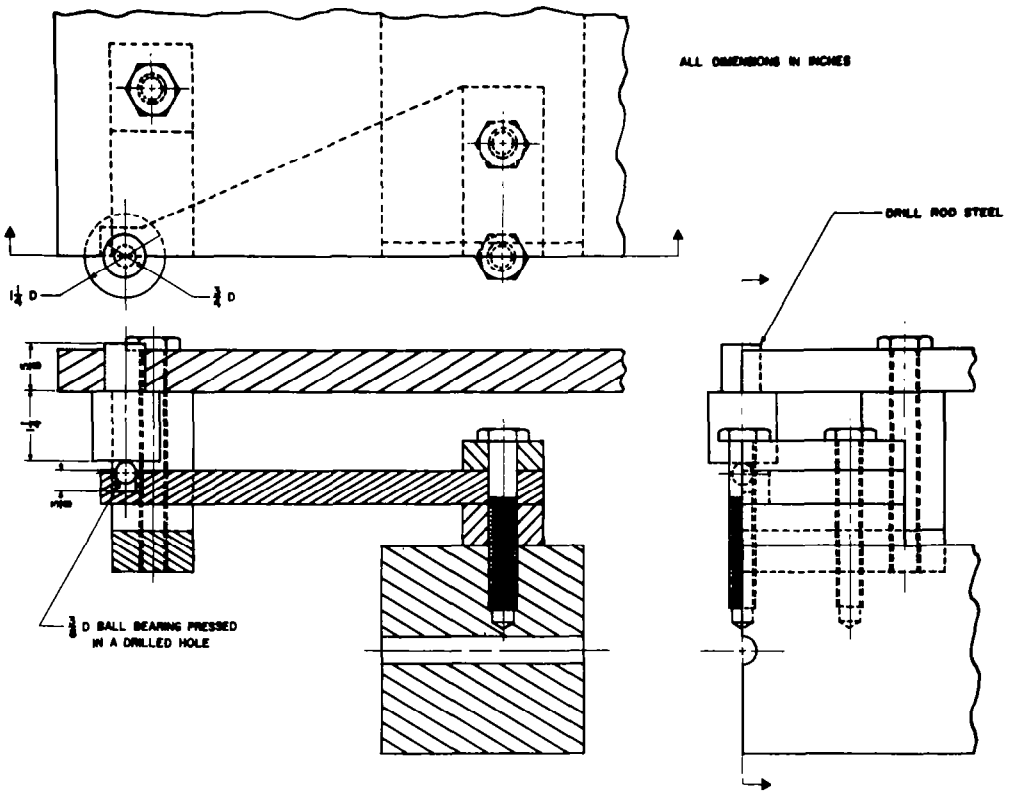

Figure 26 - Sectional View of Strain-Beam Assembly

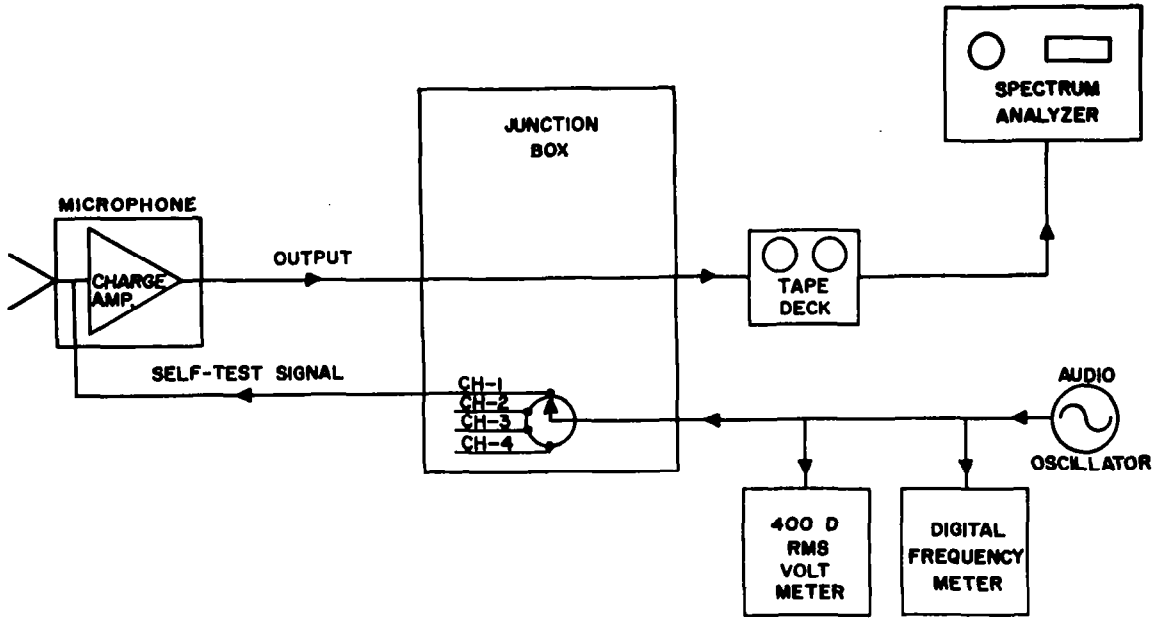

Figure 27 - Microphone Calibration Circuit

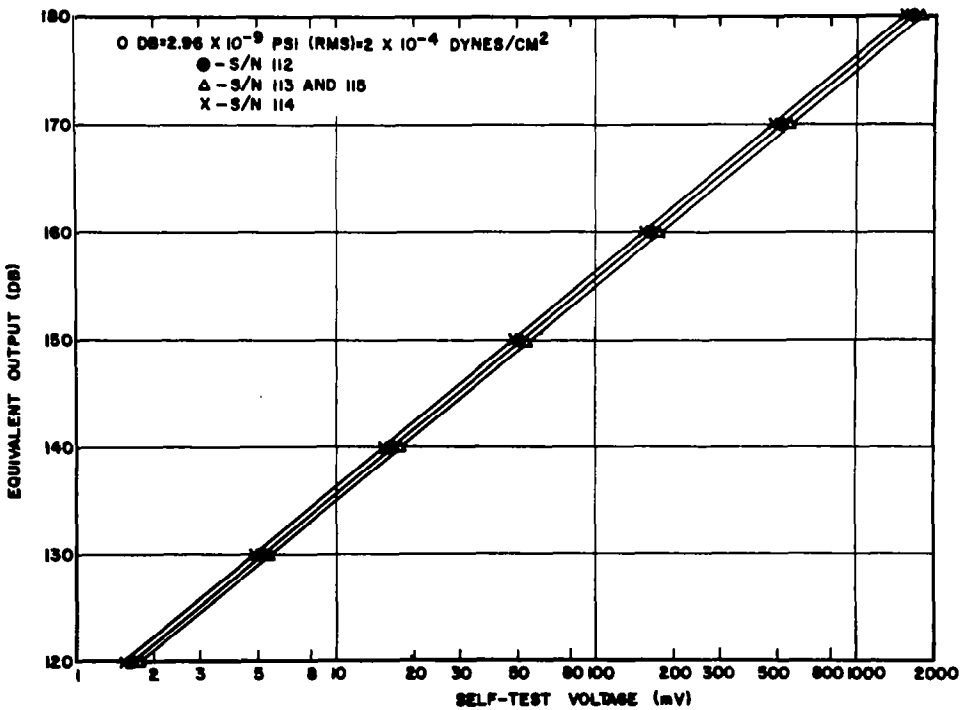

Figure 28 - Calibrated Output from Microphone

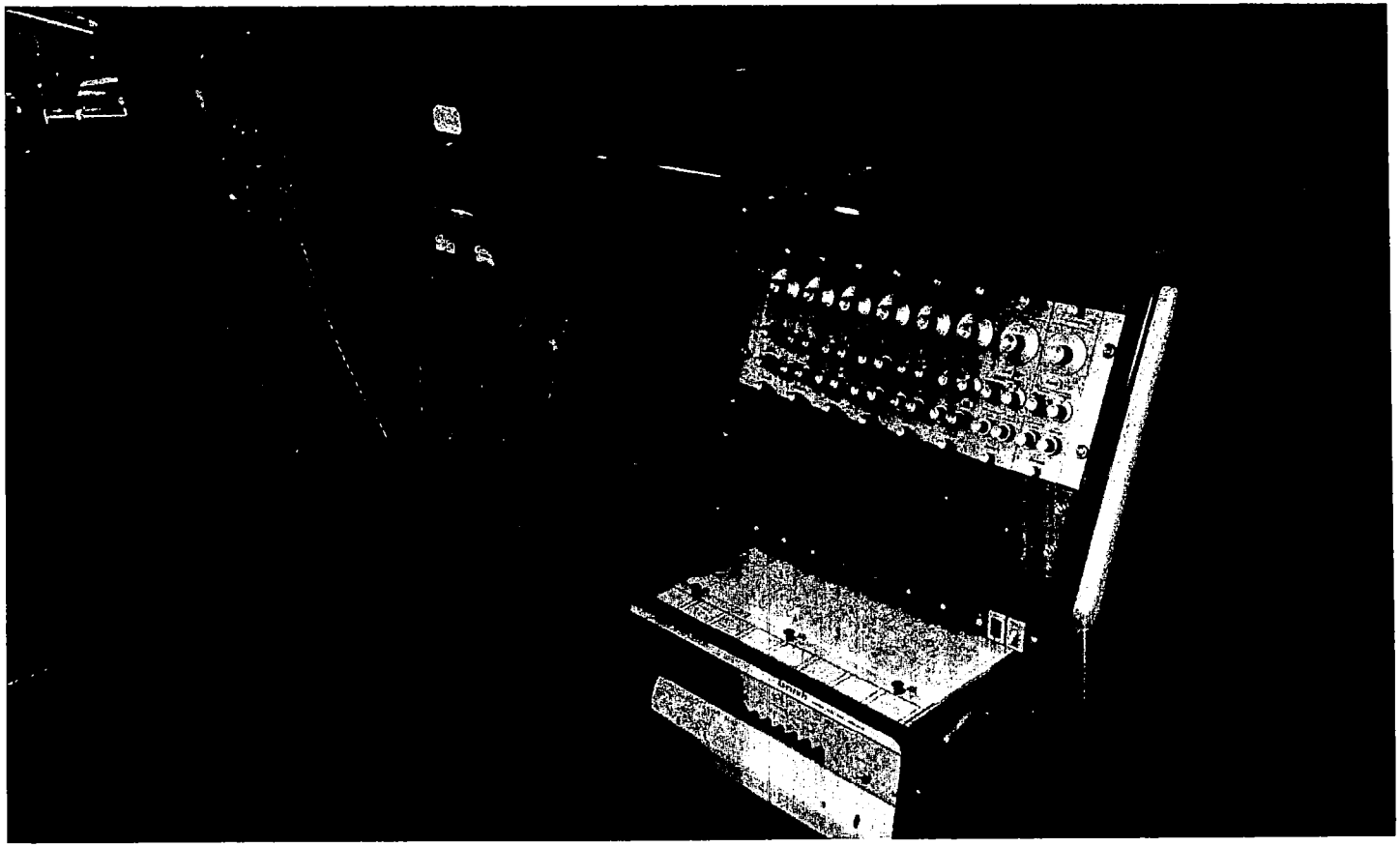

Figure 29 - Recording and Analysis Instrumentation

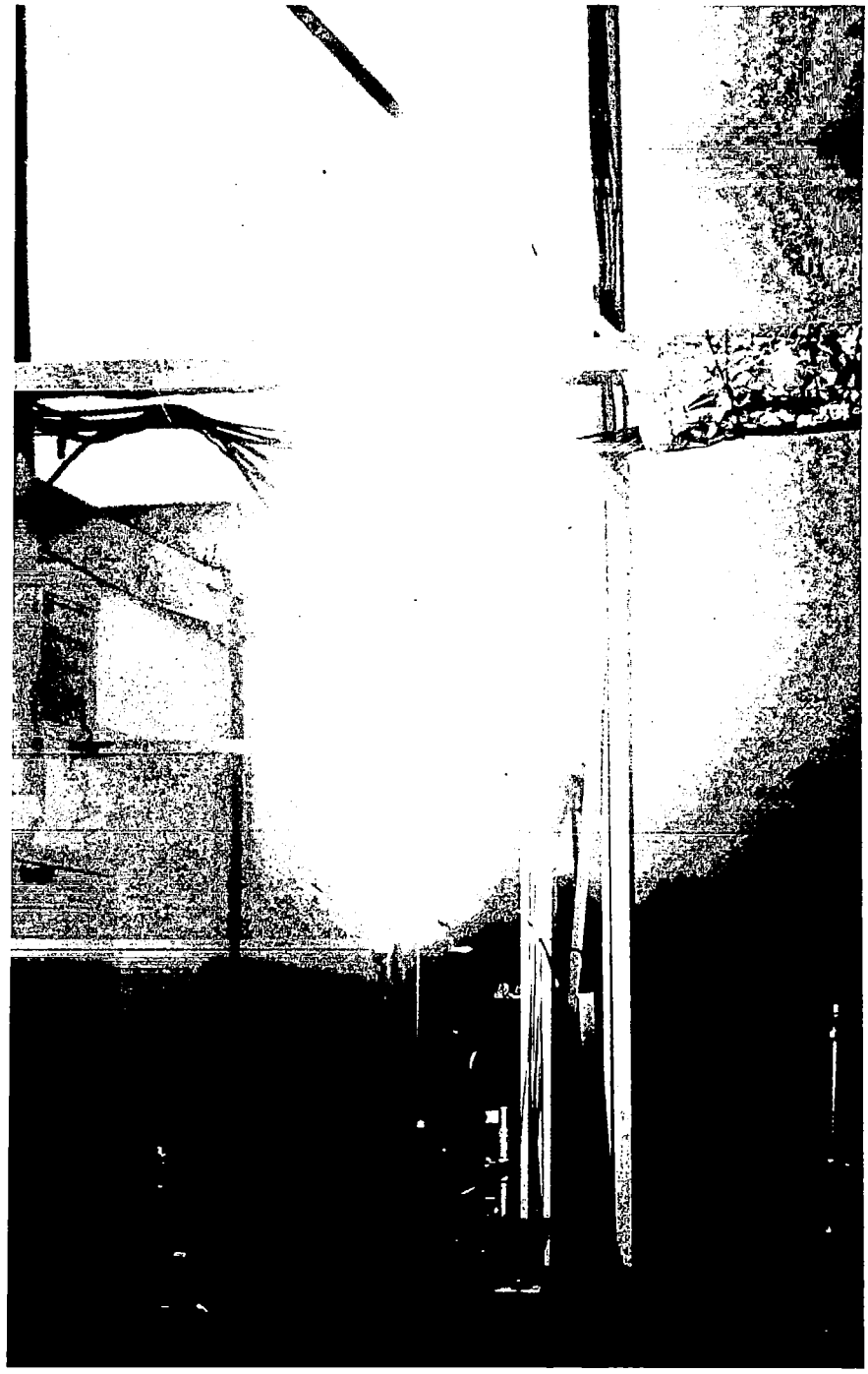

Figure 30 - Typical Rocket Experiment; Microphones are on Stands

Figure 31 - Typical Rocket Experiment

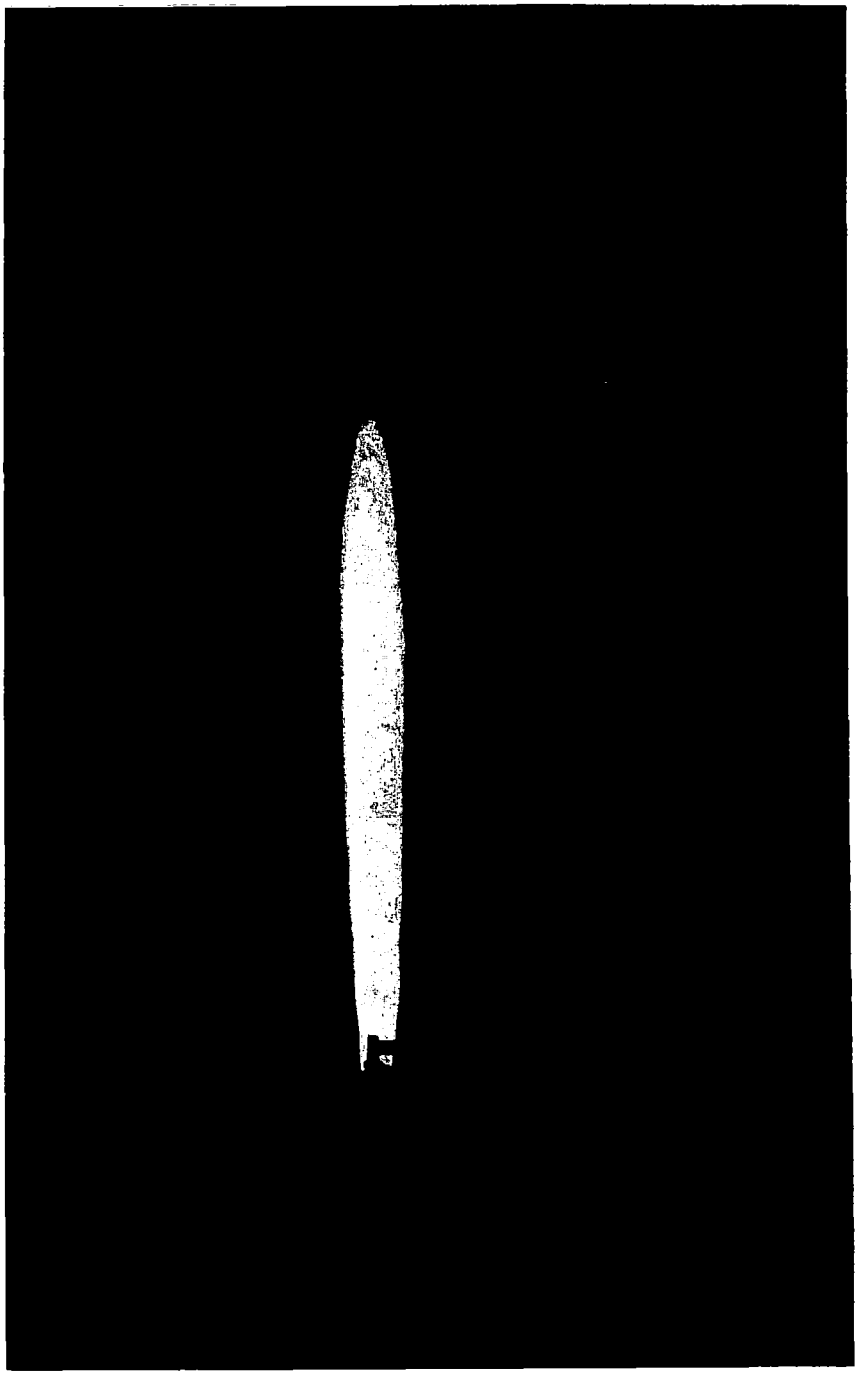

Figure 32 - Rocket Experiment; Film Exposed to Show Shock Patterns

Figure 33 - Rocket Experiment During Initiation Phase

Figure 34 - Rocket Experiment

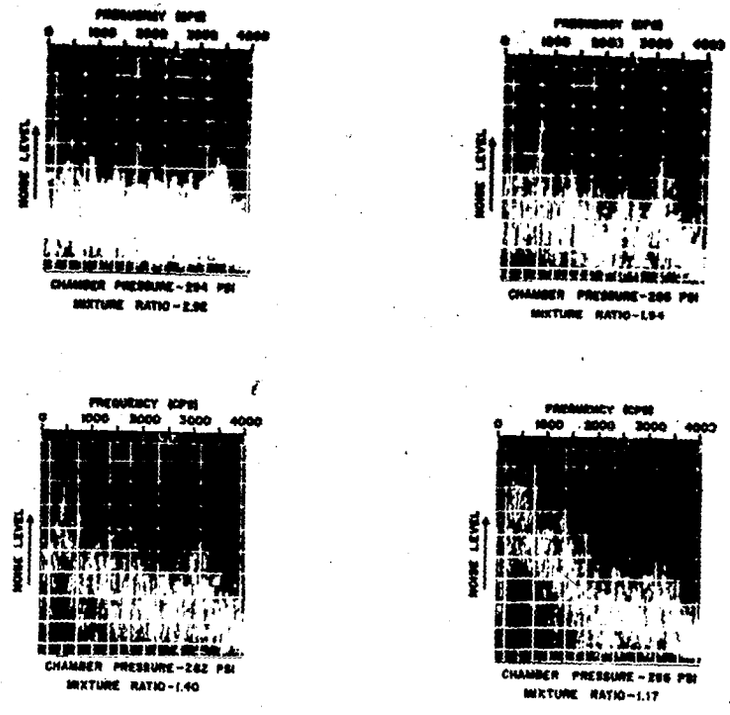

Figure 35 - Noise Spectra - Experiment 26

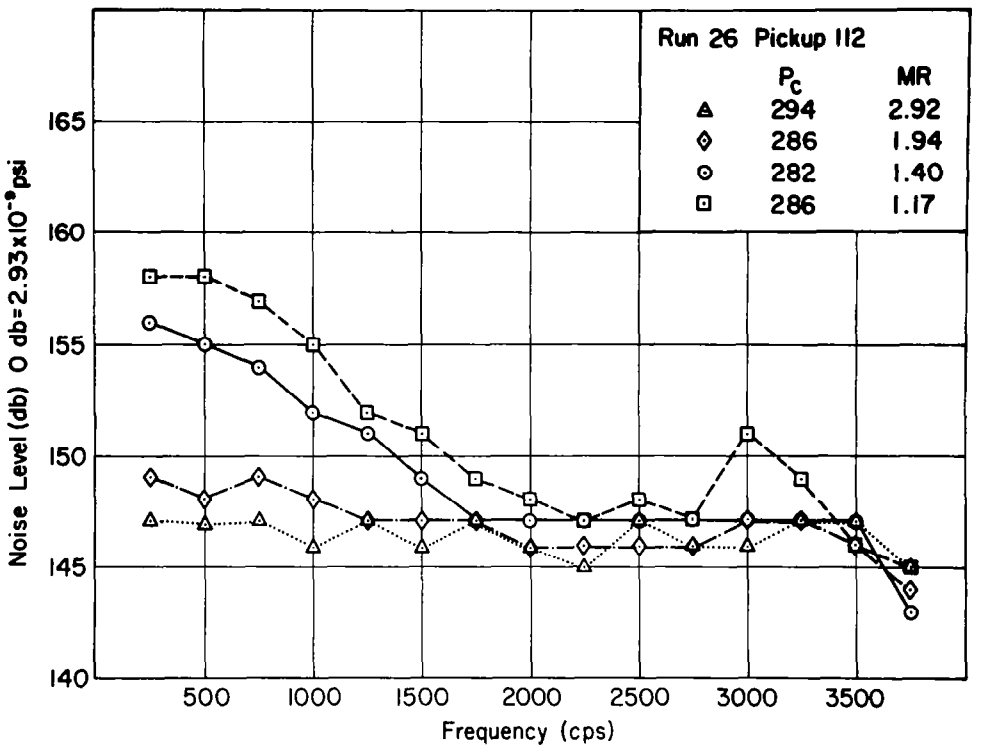

Figure 36 - Average Value of Noise Level Versus Frequency for Experiment 26; Microphone number 112

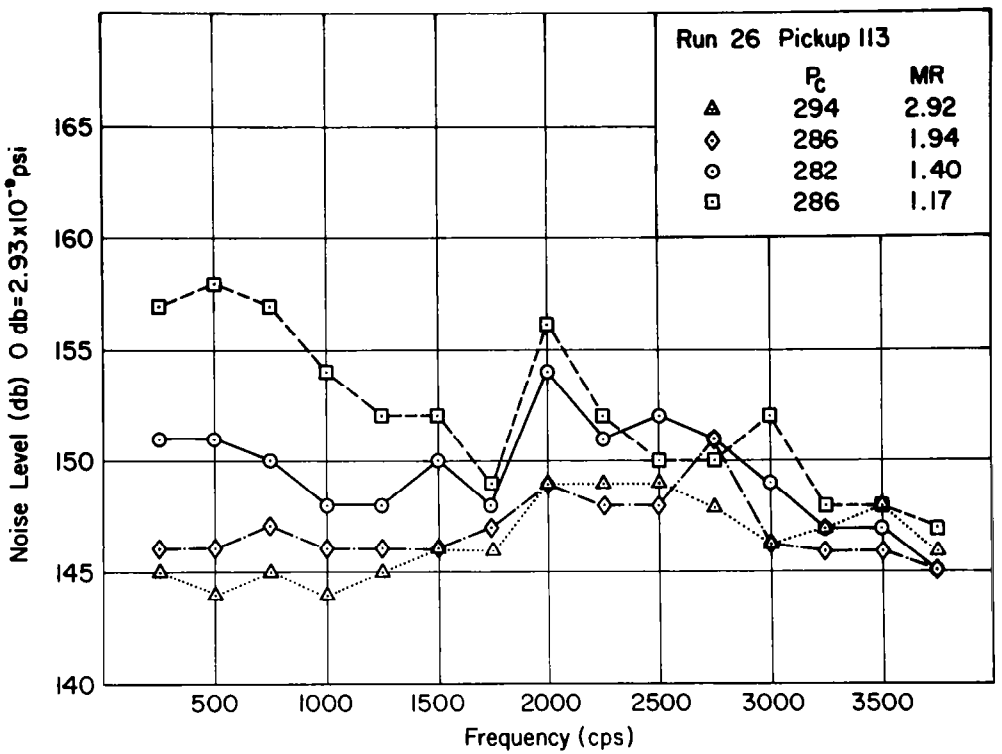

Figure 37 - Average Value of Noise Level Versus Frequency for Experiment 26; Microphone Number 113

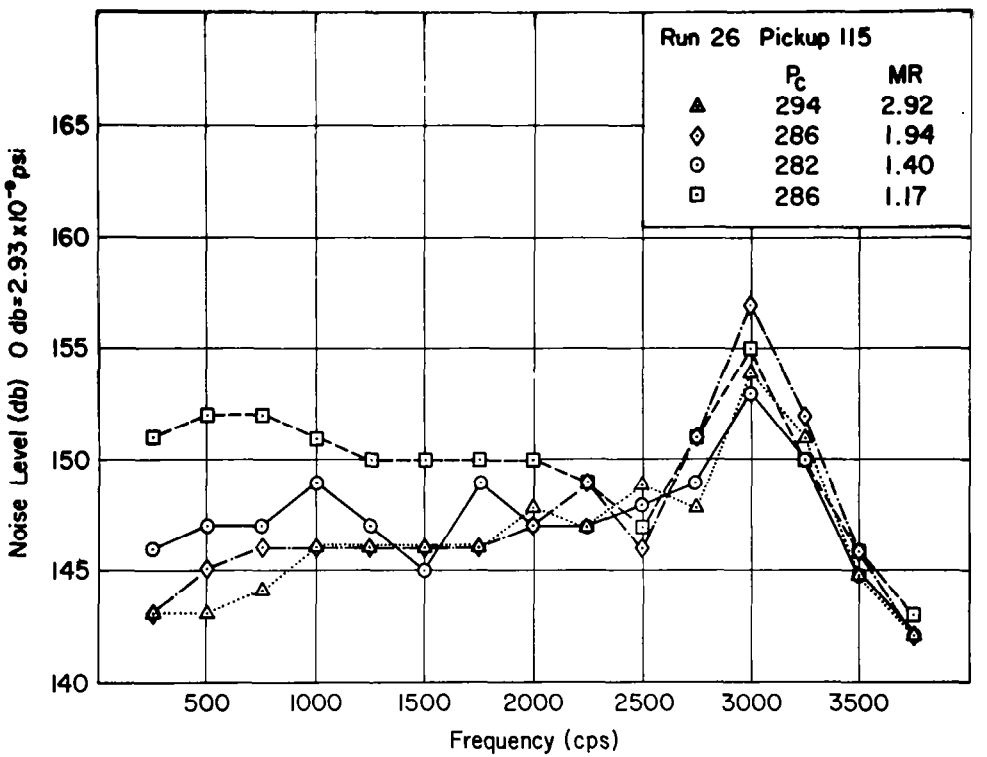

Figure 38 - Average Value of Noise Level Versus Frequency for Experiment 26; Microphone Number 115

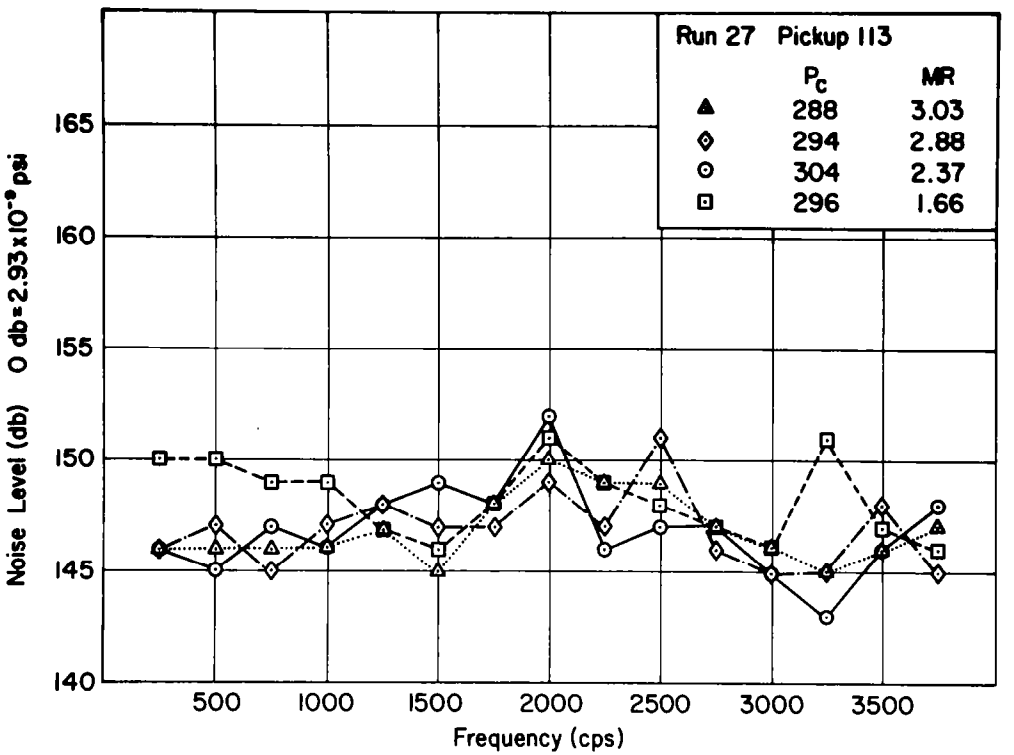

Figure 39 - Average Value of Noise Level Versus Frequency for Experiment 27; Microphone Number 113

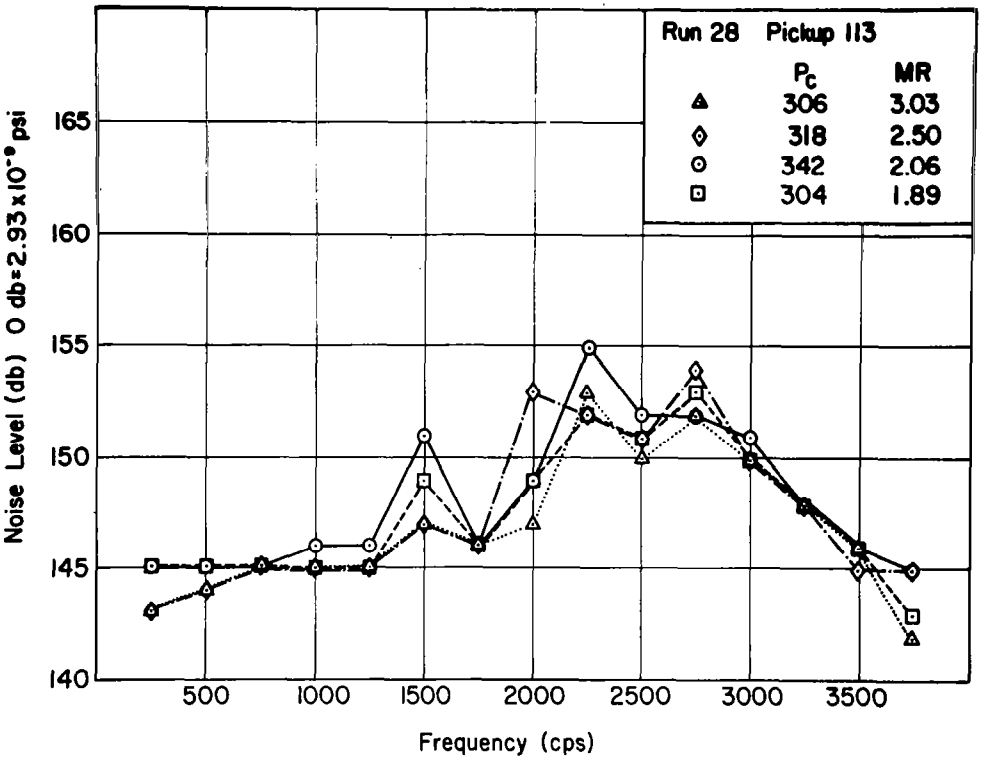

Figure 40 - Average Value of Noise Level Versus Frequency for Experiment 28 ; Microphone Number 113

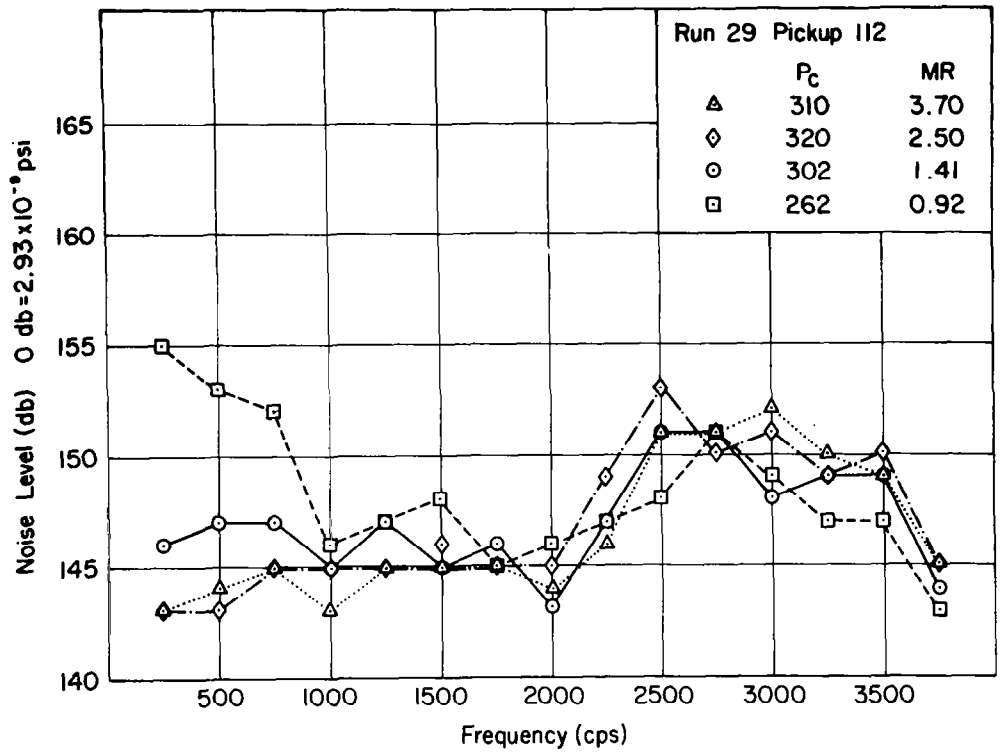

Figure 41 - Average Value of Noise Level Versus Frequency for Experiment 29; Microphone Number 112

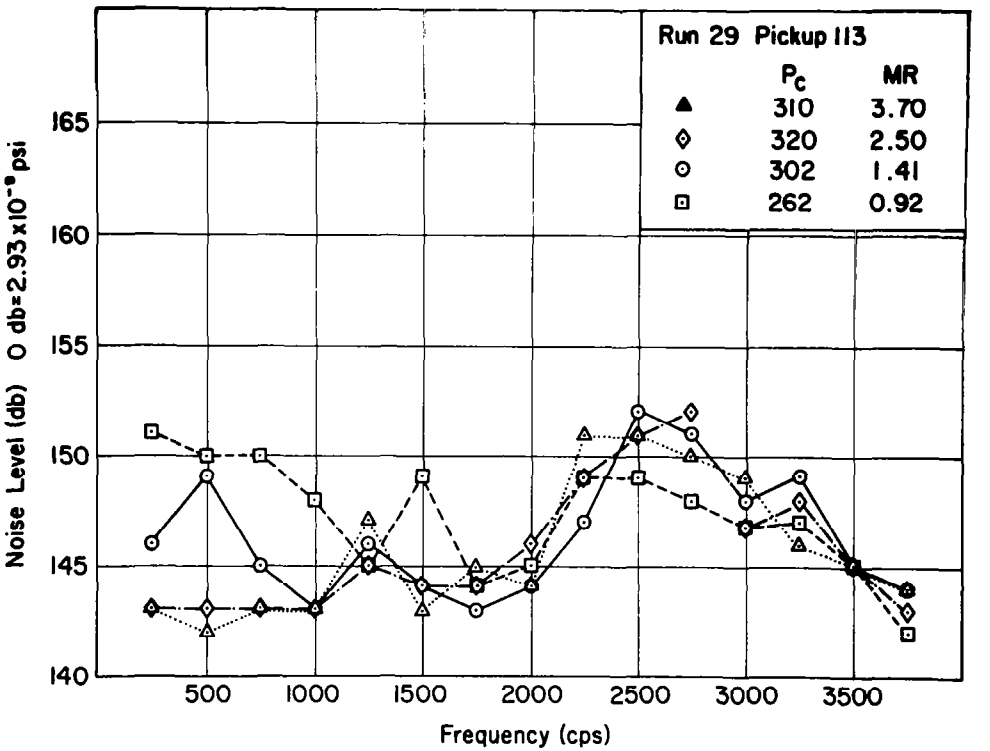

Figure 42 - Average Value of Noise Level Versus Frequency for Experiment 29; Microphone Number 113

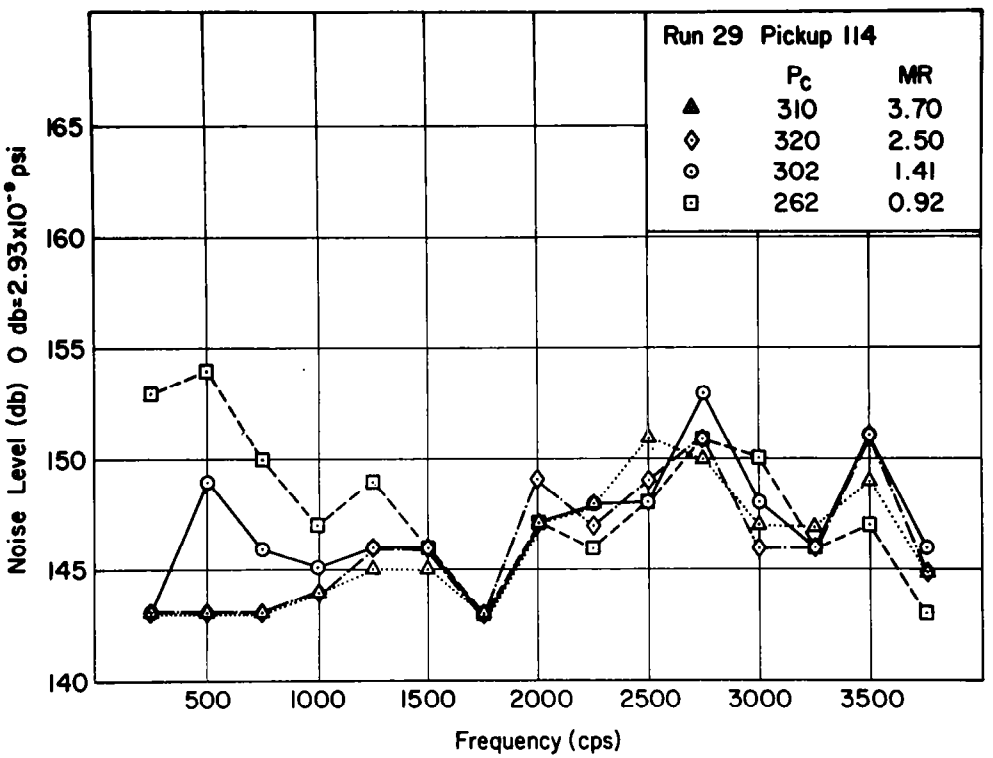

Figure 43 - Average Value of Noise Level Versus Frequency for Experiment 29; Microphone Number 114

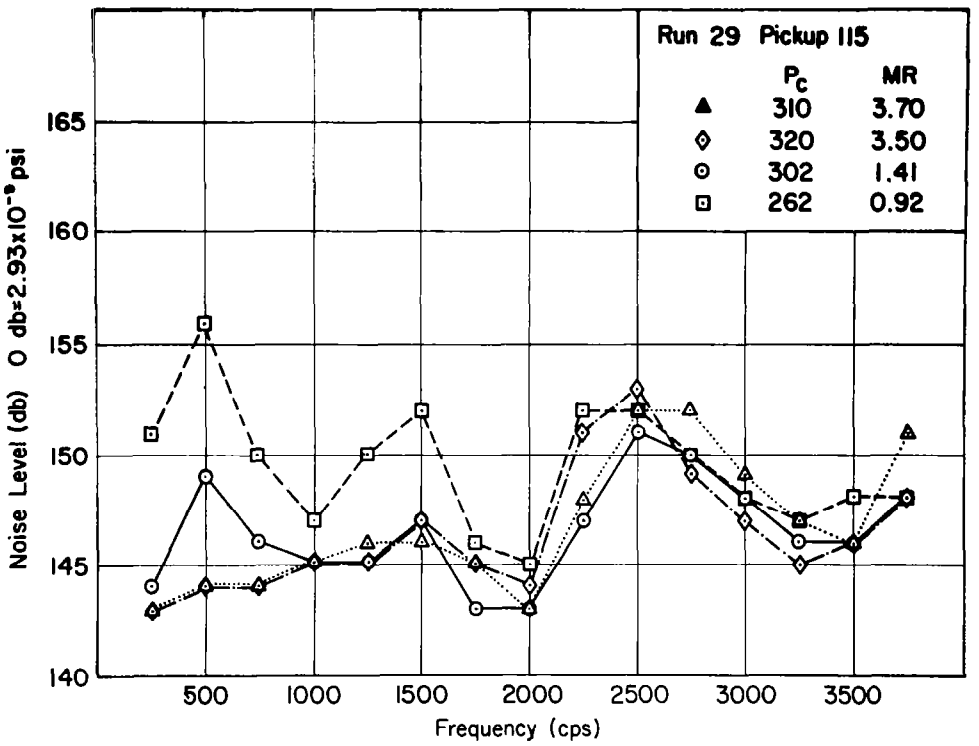

Figure 44 - Average Value of Noise Level Versus Frequency for Experiment 29; Microphone Number 115